

# TRIM28 is a distinct prognostic biomarker that worsens the tumor immune microenvironment in lung adenocarcinoma

Jie Liu<sup>1</sup>, Xiao Han<sup>2</sup>, Lijuan Chen<sup>1</sup>, Dong Han<sup>3</sup>, Xiaoqian Mu<sup>1</sup>, Xiufeng Hu<sup>1</sup>, Hongbo Wu<sup>1</sup>, Huijuan Wu<sup>1</sup>, Wenjing Liu<sup>1</sup>, Yanqiu Zhao<sup>1</sup>

<sup>1</sup>Department of Internal Medicine, The Affiliated Tumor Hospital of Zhengzhou University, Zhengzhou, China

<sup>2</sup>Department of Obstetrics and Gynecology, The Third Affiliated Hospital of Zhengzhou University, Zhengzhou, China

<sup>3</sup>Department of Oncology, The First Affiliated Hospital of Zhengzhou University, Zhengzhou, China

Correspondence to: Yanqiu Zhao; email: [zlyyliujie2791@zzu.edu.cn](mailto:zlyyliujie2791@zzu.edu.cn)

Keywords: TRIM28, tumor immune microenvironment, lung adenocarcinoma, prognosis

Received: April 20, 2020

Accepted: July 9, 2020

Published: October 22, 2020

Copyright: © 2020 Liu et al. This is an open access article distributed under the terms of the [Creative Commons Attribution License](https://creativecommons.org/licenses/by/3.0/) (CC BY 3.0), which permits unrestricted use, distribution, and reproduction in any medium, provided the original author and source are credited.

## ABSTRACT

The tumor immune microenvironment (TIME) is an important determinant of cancer prognosis and treatment efficacy. To identify immune-related prognostic biomarkers of lung adenocarcinoma, we used the ESTIMATE algorithm to calculate the immune and stromal scores of 517 lung adenocarcinoma patients from The Cancer Genome Atlas (TCGA). We detected 985 differentially expressed genes (DEGs) between patients with high and low immune and stromal scores, and we analyzed their functions and protein-protein interactions. *TRIM28* was upregulated in lung adenocarcinoma patients with low immune and stromal scores, and was associated with a poor prognosis. The TISIDB and TIMER databases indicated that *TRIM28* expression correlated negatively with immune infiltration. We then explored genes that were co-expressed with *TRIM28* in TCGA, and investigated DEGs based on *TRIM28* expression in GSE43580 and GSE7670. The 429 common DEGs from these analyses were functionally analyzed. We also performed a Gene Set Enrichment Analysis using TCGA data, and predicted substrates of *TRIM28* using UbiBrowser. The results indicated that *TRIM28* may negatively regulate the TIME by increasing the SUMOylation of IRF5 and IRF8. Correlation analyses and validations in two lung adenocarcinoma cell lines (PC9 and H1299) confirmed these findings. Thus, *TRIM28* may worsen the TIME and prognosis of lung adenocarcinoma.

## INTRODUCTION

Lung cancer is still the most common form of cancer and the leading cause of cancer death worldwide in both developing and developed regions [1]. Non-small-cell lung cancer (NSCLC) accounts for 85% of lung cancer cases, and can be classified as adenocarcinoma, squamous cell carcinoma or large cell carcinoma. Lung adenocarcinoma (LUAD) is one of the most common subtypes of NSCLC [2], and has been extensively studied in recent years due to the great success of molecular targeted therapy.

Immune evasion is acknowledged as a hallmark of tumors [3], and different immune cell types contribute to immune infiltration and immune evasion. Immunotherapies such as programmed cell death-1 (PD1) / programmed cell death ligand-1 (PD-L1) inhibitors have become standard-of-care treatment options for NSCLC patients. However, only a small subset (20-30%) of patients respond to such treatments [4-7]. At present, the prognosis of LUAD remains poor, and the overall five-year survival rate is < 15% due to local and distant recurrences [8].

Tumor-infiltrating lymphocytes and neutrophils are known to influence the prognosis of cancers and the

efficacy of antitumor therapies [9, 10]. The level of infiltrating stromal and immune cells in tumor samples can be predicted with the ESTIMATE (Estimation of STromal and Immune cells in MAlignant Tumor tissues using Expression data) algorithm, which calculates immune and stromal scores based on unique gene signatures. Two main gene signatures are used: one based on 141 stroma-related genes that reflect the presence of stroma in tumor tissues, and the other based on 141 immune-related genes that represent the infiltration of immune cells into tumor tissues [11]. The current knowledge about the link between the tumor immune microenvironment (TIME) and LUAD is insufficient. Therefore, there is an urgent need to better understand tumor-immune interactions and identify more precise prognostic predictors and molecular biomarkers for lung cancer.

Tripartite motif-containing (TRIM) proteins, which include a structurally conserved RING-finger domain, one or two B-box zinc finger domains and a coiled-coil domain, are considered to be significant regulators of carcinogenesis [12]. TRIM28 (also known as KAP1, TIF1 $\beta$  or KRIP1), one of the 60 members of the TRIM family, is a small ubiquitin-like modifier (SUMO) E3 ligase and a fundamental component of several macromolecular complexes [13–15]. TRIM28 is a poorly understood transcriptional co-factor with pleiotropic biological activities, including inducing gene silencing, promoting cellular proliferation and differentiation, promoting neoplastic transformation, inhibiting apoptosis, facilitating DNA repair, and guarding genomic integrity [16]. TRIM28 also promotes T cell activation, T cell tolerance, and the expression of various interleukins and other pro-inflammatory molecules [17–25]. The upregulation of TRIM28 predicts a poor prognosis in patients with gastric cancer [26], ovarian cancer [27], breast cancer [12] and colorectal cancer [28]. Lei et al. [29] found that the upregulation of TRIM28 promoted the growth of NSCLC and was a potential predictor of metastasis and prognosis in early-stage NSCLC patients. However, Chen et al. [30] reported that TRIM28 exerted anti-proliferative activity in lung cancer by repressing E2F family members that are critical for cell proliferation. Due to these contradictory observations, the prognostic value of TRIM28 in lung cancer remains unclear.

In this study, we conducted a comprehensive analysis of immune cell infiltration and gene expression in the TIME of LUAD based on the ESTIMATE algorithm, and then correlated these data with clinical and prognostic features. The results revealed the significant prognostic value of *TRIM28* expression and a potential mechanism whereby TRIM28 alters the TIME in LUAD.

## RESULTS

### The correlations among the immune and stromal scores, clinical features and prognoses of LUAD patients

The overall flowchart of this study is shown in Figure 1. In total, 517 LUAD patients with RNA sequencing data and clinical information in The Cancer Genome Atlas (TCGA) database were included (<http://www.cbioportal.org>, Firehose Legacy, Supplementary Table 1) [31]. Patients' immune and stromal scores were determined using the ESTIMATE algorithm based on gene expression data [11]. The detailed results are presented in Supplementary Table 2.

After comprehensively analyzing the stromal and immune scores, clinical information and RNA sequencing data, we found that both the stromal and immune scores were significantly lower in men ( $p = 0.009$ ,  $p = 0.005$ , respectively; Figure 2A and 2B), in patients with higher *TRIM28* expression ( $p < 0.001$ ,  $p < 0.001$ ; Figure 2C and 2D) and in patients with metastasis ( $p = 0.007$ ,  $p = 0.035$ ; Figure 2K and 2L) than in their respective counterpart groups. In addition, the immune scores were lower in patients in higher tumor-node-metastasis (TNM) stages and T stages ( $p = 0.036$ ,  $p = 0.005$ ; Figure 2F and 2H). However, the stromal scores did not correlate with the TNM stages or T stages ( $p = 0.107$ ,  $p = 0.286$ ; Figure 2E and 2G). The stromal and immune scores also did not correlate significantly with the lymph node metastasis status ( $p = 0.746$ ,  $p = 0.439$ ; Figure 2I and 2J).

Patients were then divided into two groups according to the median value of the stromal score or the immune score. Then, overall survival (OS) (Figure 2M and 2N) and disease-free survival (DFS) (Figure 2O and 2P) were compared between the respective groups. OS was worse in patients with lower stromal scores or immune scores than in those with higher scores ( $p = 0.059$ ,  $p = 0.009$ ). However, DFS did not differ significantly between the respective groups.

### Identification and functional annotation of differentially expressed genes

Next, we examined the differentially expressed genes (DEGs) between patients with high and low stromal scores, as shown in the heatmap in Figure 3A. We found that 1,401 genes were upregulated in the group with high stromal scores, while 448 genes were upregulated in the group with low stromal scores. We also evaluated the DEGs between patients with high and low immune scores (Figure 3B), and found that 1,278 genes were upregulated in the group with high immune scores, while 278 genes were upregulated in the group with low immune scores.

Then, using an online tool (<http://bioinformatics.psb.ugent.be/webtools/Venn/>), we generated Venn diagrams to identify overlapping DEGs (Figure 3C and 3D). The results indicated that 872 genes were commonly upregulated in the groups with high stromal scores and high immune scores, while 113 genes were commonly upregulated in the groups with low stromal scores and low immune scores.

To explore the biological functions of the 985 DEGs, we performed Gene Ontology (GO) and Kyoto Encyclopedia of Genes and Genomes (KEGG) analyses using Metascape [32]. The top 15 GO enrichment terms and KEGG enrichment terms are shown in Figure 3F and 3G, respectively. Most of the terms were related to immune regulation, including lymphocyte activation, regulation of cytokine production, interferon production, etc.

Considering the poor prognoses of patients with low stromal or immune scores, we then performed a protein-

protein interaction (PPI) analysis on the 113 genes that were commonly upregulated in patients with low stromal and immune scores (Figure 3E). The top 15 genes identified using the maximal clique centrality method were chosen as hub genes through the cytoHubba plugin: *ARHGEF16*, *ESRP1*, *TRIM28*, *RBBP8NL*, *CLDN7*, *RAB25*, *APIM2*, *EPCAM*, *LLGL2*, *KDF1*, *OVOL2*, *FAM83H*, *EPN3*, *CAMSAP3* and *SHMT1* (Figure 3H). Interestingly, other methods in the cytoHubba plugin also identified *TRIM28* as a crucial hub gene (Supplementary Table 3).

### The mRNA and protein levels of TRIM28 across cancer types

To determine whether *TRIM28* expression differed between tumor tissues and healthy tissues, we used the Oncomine database to analyze *TRIM28* mRNA levels in multiple cancer types. *TRIM28* expression was higher in bladder cancer, colorectal cancer, gastric cancer, head

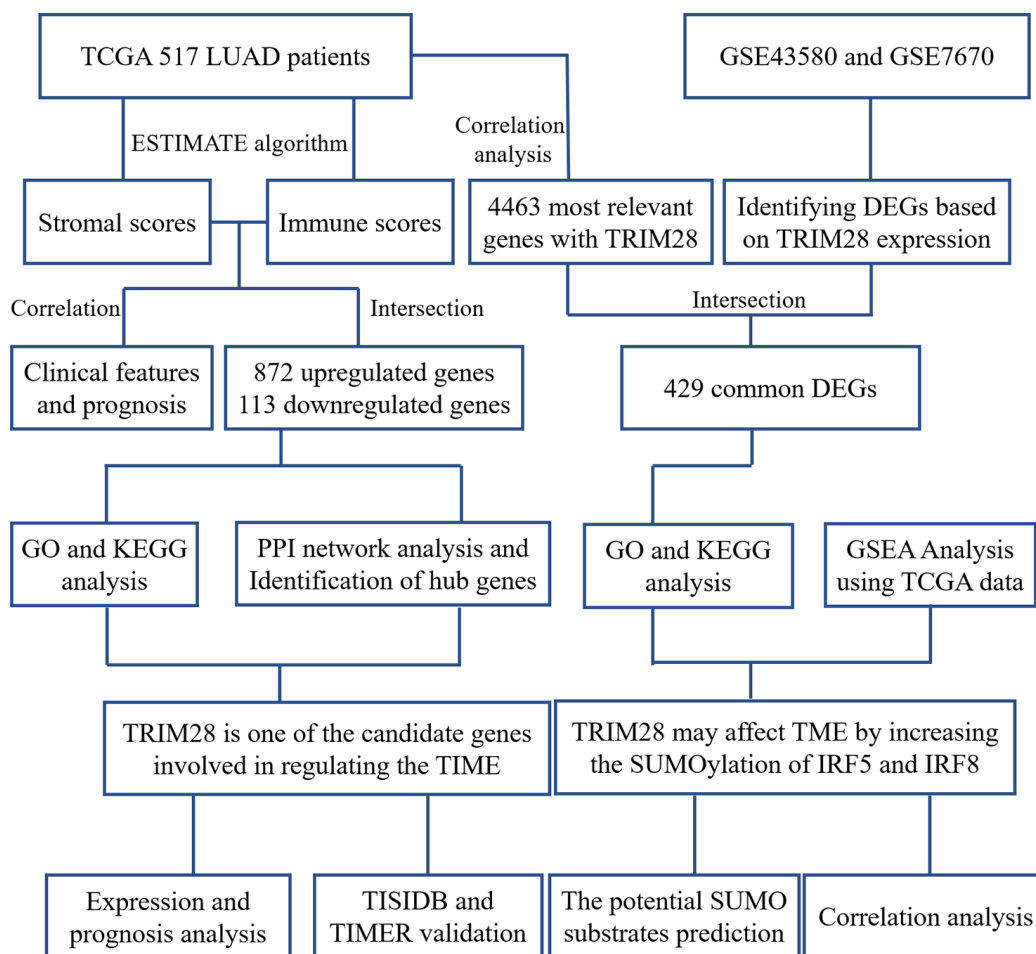


**Figure 1. Workflow of the present study.** TCGA, The Cancer Genome Atlas; LUAD, lung adenocarcinoma; PPI, protein-protein interaction; GSE, Gene Expression Omnibus data series; DEGs, differentially expressed genes; TIME, tumor immune microenvironment.

and neck cancer, liver cancer, lung cancer and multiple myeloma than in healthy tissues (Figure 4A). We also examined *TRIM28* RNA levels in various tumor tissues and adjacent healthy tissues using the RNA sequencing data in TCGA (Figure 4B). *TRIM28* was significantly upregulated in most of the tumor tissues, including bladder urothelial carcinoma, breast invasive carcinoma, LUAD, lung squamous cell carcinoma, etc. However, *TRIM28* RNA levels were significantly lower in kidney renal papillary cell carcinoma than in adjacent healthy tissues. The significant increase in *TRIM28* expression in LUAD was further validated in four independent data sets, including GSE32863 [33], GSE7670 [34], GSE19188 [35] and the Beer Lund dataset [36] (Figure 4C–4F).

We also used the UALCAN cancer database to examine *TRIM28* protein levels in various cancer tissues. *TRIM28* protein expression was upregulated in breast cancer, colon cancer, ovarian cancer, clear cell renal cell carcinoma, uterine corpus endometrial carcinoma and LUAD (Figure 4G).

### Prognostic value of *TRIM28* across cancer types

We then used the PrognoScan database to investigate whether *TRIM28* expression correlated with the prognosis of cancer patients. Notably, *TRIM28* expression significantly impacted the prognosis of seven cancer types, including breast, lung, ovarian, brain, skin, prostate and blood cancers (Figure 5A–5L).

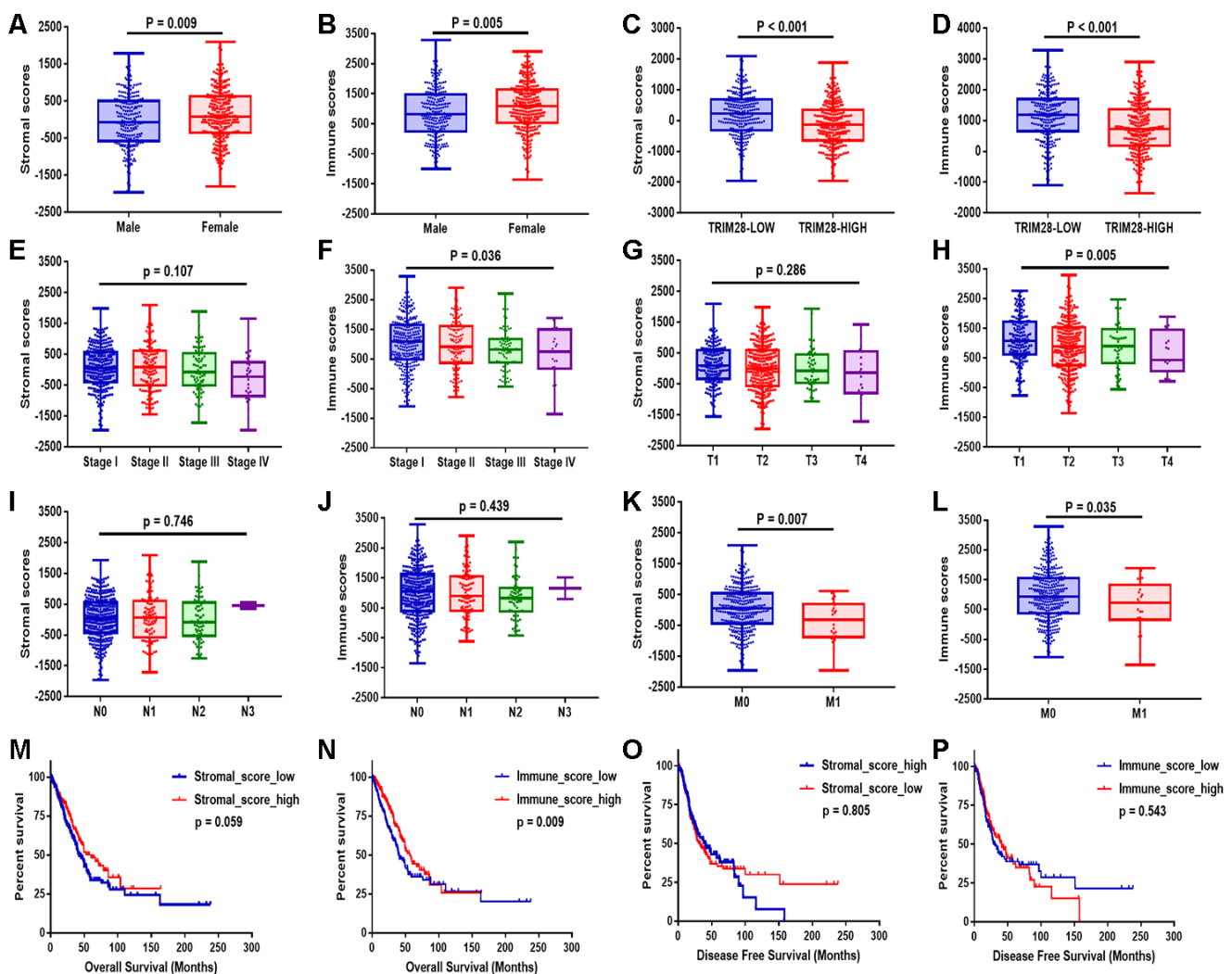


**Figure 2. Stromal and immune scores were associated with the clinical characteristics and OS of LUAD patients.** (A–L) The stromal and immune score distributions between patients with different genders (A, B), TRIM28 levels (C, D), TNM stages (E, F), T classifications (G, H), lymph node metastasis statuses (I, J) and distant metastasis statuses (K, L). (M–P) Patients were then divided into two groups according to the median stromal score or immune score. OS (M, N) and DFS (O, P) analyses were performed between the respective groups. OS, overall survival; LUAD, lung adenocarcinoma.

In three cohorts (GSE4922-GPL96, GSE3494-GPL96 and GSE7378) [37–39] that respectively included 249 samples, 236 samples and 54 cases at different stages of breast cancer, higher *TRIM28* expression was

marginally associated with poorer DFS or disease-specific survival (DSS) (DFS hazard ratio [HR] = 3.62, 95% confidence interval [CI] = 2.03 to 6.44, Cox  $p < 0.001$ ; DSS HR = 3.76, 95% CI = 1.77 to 7.98, Cox

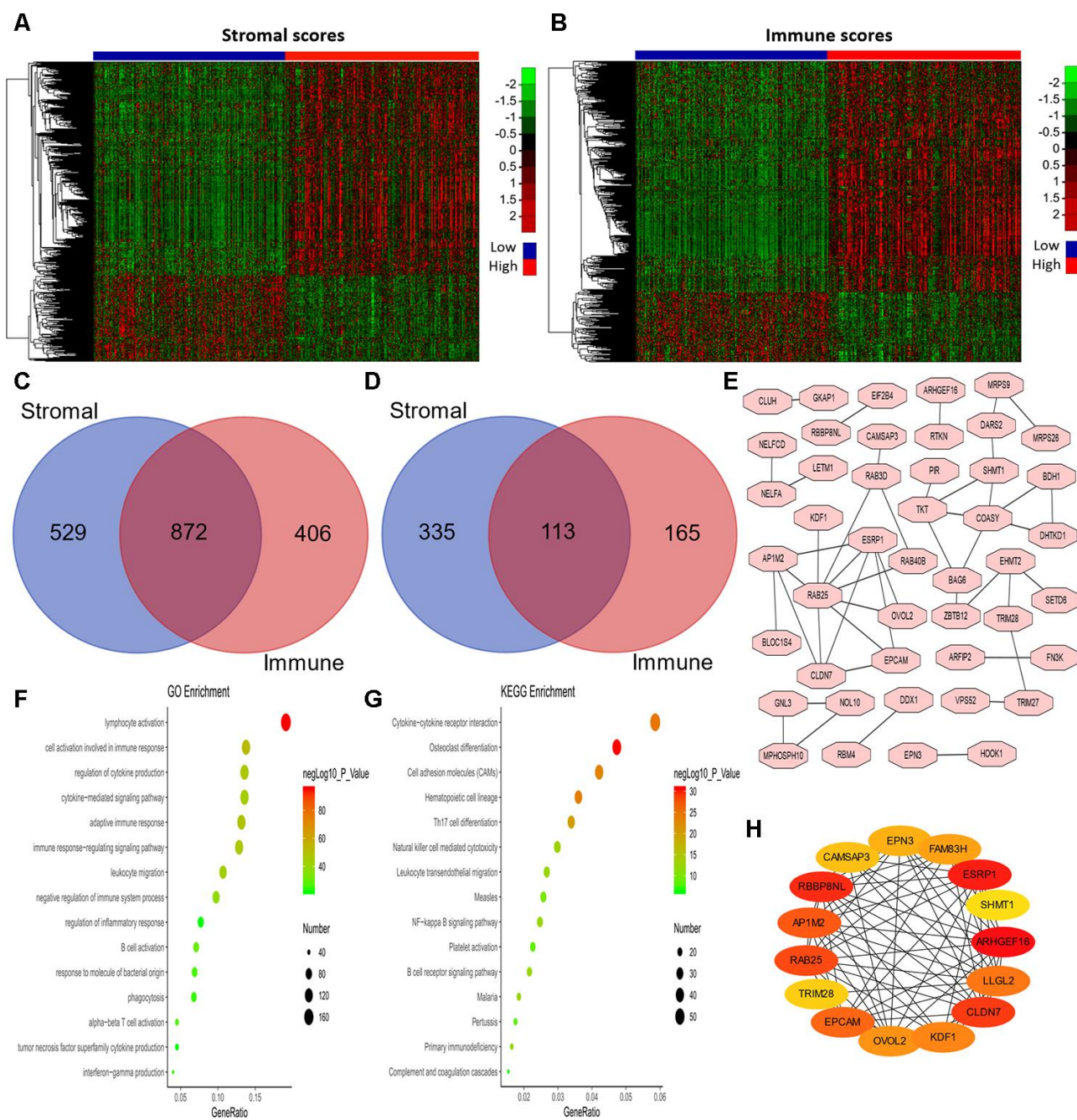


**Figure 3. Analysis of DEGs according to the immune and stromal scores in LUAD patients.** (A, B) Clustering Heatmap plot of the DEGs. The upper color bar represents the sample class; red represents the group with higher scores, while blue represents the group with lower scores. Genes with higher levels are shown in red, while those with lower levels are shown in green. (C, D) Venn diagrams showing the number of commonly upregulated (C) or downregulated (D) DEGs. (E) PPI analysis of downregulated DEGs via STRING. The interaction score was set to medium confidence (0.400). (F, G) The top 15 GO enrichment terms (F) and KEGG enrichment terms (G) for all DEGs, analyzed in Metascape. (H) The first 15 genes identified through the maximal clique centrality method were chosen as hub genes using the cytoHubba plugin. More red color represents more forward ranking. GO, gene ontology; KEGG, Kyoto Encyclopedia of Genes and Genomes; DEGs, differentially expressed genes; LUAD, lung adenocarcinoma; MMC, maximal clique centrality.

$p < 0.001$ ; DFS HR = 104.71, 95% CI = 6.95 to 1577.65, Cox  $p < 0.001$ ; Respectively; Figure 5A–5C). However, in two other cohorts (GSE9893 and GSE11121) [40, 41] that respectively included 155 and 200 samples at different stages of breast cancer, lower *TRIM28* expression was associated with poorer OS or distant metastasis-free survival (DMFS) (OS HR = 0.80, 95% CI = 0.68 to 0.95, Cox  $p = 0.008$ ; DMFS HR = 0.34, 95% CI = 0.13 to 0.89, Cox  $p = 0.028$ ; Respectively; Figure 5D, 5E). In one cohort (GSE31210) [42] that included 204 samples at different stages of

LUAD, higher *TRIM28* expression was marginally associated with poorer recurrence-free survival (RFS) and OS (RFS HR = 5.44, 95% CI = 2.73 to 10.87, Cox  $p < 0.001$ ; OS HR = 3.59, 95% CI = 1.33 to 9.68, Cox  $p = 0.012$ ; Figure 5F and 5G). We also observed the poor prognostic value of *TRIM28* in brain cancer, prostate cancer, blood cancer and renal cell carcinoma (Figure 5H, 5J–5L) and its good prognostic value in ovarian cancer (Figure 5I). These results suggested that *TRIM28* expression influences the prognosis of LUAD and other tumor types.

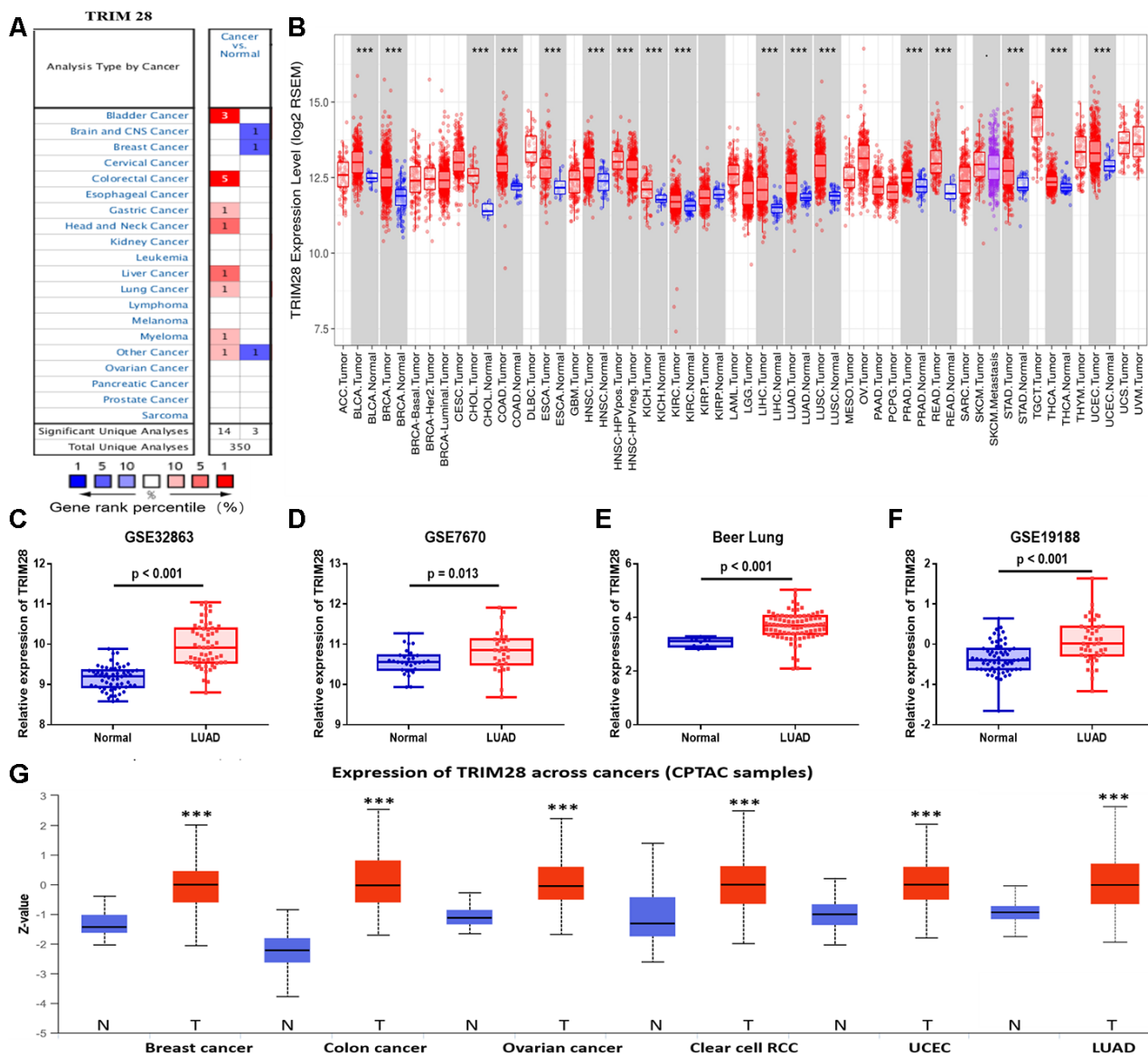


**Figure 4. TRIM28 levels in different human cancer types.** (A) Increased or reduced TRIM28 levels in different cancers compared with normal tissues in the Oncomine database. (B) Human TRIM28 levels in different tumor types from TCGA were determined using TIMER. (C–F) The significant increase in TRIM28 expression in LUAD was further validated in GSE32863 (C), GSE7670 (D), the Beer Lung dataset (E) and GSE19188 (F). (G) The protein expression of TRIM28 in various cancer tissues was detected using the UALCAN cancer database ( $*p < 0.05$ ,  $**p < 0.01$ ,  $***p < 0.001$ ). TCGA, The Cancer Genome Atlas; LUAD, lung adenocarcinoma; UCEC, uterine corpus endometrial carcinoma; GSE, Gene Expression Omnibus data series.

To further examine the prognostic potential of *TRIM28* in different cancers based on Affymetrix microarrays, we used the Kaplan-Meier plotter database. Higher *TRIM28* expression was associated with a poorer prognosis in lung cancer and gastric cancer. However, *TRIM28* expression had less of an impact on the

prognosis of ovarian cancer and breast cancer (Supplementary Figure 1). These results confirmed the significant prognostic value of *TRIM28* expression in lung cancer and gastric cancer. We also analyzed the prognostic potential of *TRIM28* in 33 different cancer types by using Gene Expression Profiling Interactive

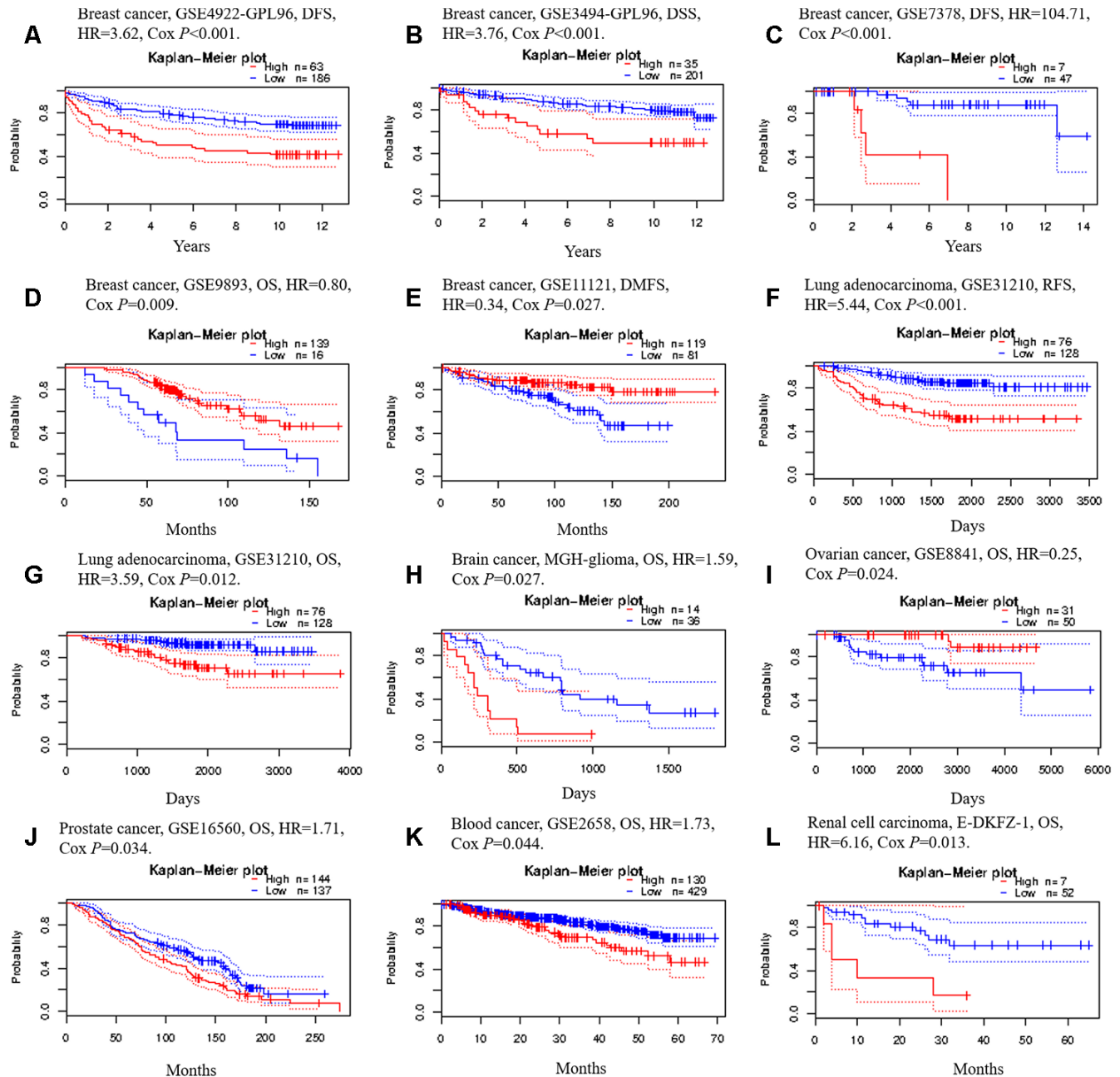


**Figure 5. Kaplan-Meier survival curves generated from the PrognScan database for *TRIM28* expression in different tumor types. (A–E) DFS, DSS, DMFS and OS curves for five breast cancer cohorts (GSE4922-GPL96, GSE3494-GPL96, GSE7378, GSE9893 and GSE11121). (F, G) RFS and OS curves for lung cancer (GSE31210). (H) OS curve for brain cancer (MGH-glioma). (I) OS curve for ovarian cancer (GSE8841). (J) OS curve for prostate cancer (GSE16560). (K) OS curve for blood cancer (GSE2658). (L) OS curve for renal cell carcinoma. DFS, disease-free survival; DSS, disease-specific survival; DMFS, distant metastasis-free survival; OS, overall survival; RFS, recurrence-free survival; GSE, Gene Expression Omnibus data series; HR, hazard ratio.**

Analysis (GEPIA) to evaluate RNA sequencing data from TCGA. Higher *TRIM28* levels were associated with poorer OS in adrenocortical carcinoma, brain lower grade glioma, LUAD, mesothelioma, skin cutaneous melanoma, etc. (Supplementary Figure 2). Thus, although the prognostic value of *TRIM28* expression differed among different cancer types, the results from different databases all confirmed the prognostic value of *TRIM28* expression in LUAD.

Next, we explored the relationship between *TRIM28* expression and the clinical characteristics of lung cancer patients in the Kaplan-Meier plotter database. Over-expression of *TRIM28* was associated with worse OS and worse first progression (FP), regardless of gender and smoking history ( $p < 0.001$ ). Interestingly, when patients were analyzed according to the type of lung cancer, the upregulation of *TRIM28* was associated with worse OS and FP in LUAD (OS HR = 2.65,  $p < 0.001$ ; FP HR = 2.00,  $p < 0.001$ ), but was not associated with OS in lung squamous cell carcinoma (OS HR = 1.25,  $p = 0.095$ ). Moreover, higher *TRIM28* expression was associated with worse OS in stage 1, stage 2, stage N0 and stage M0, but was not associated with worse OS according to the grade, stage 3, stage T, stage N1 or stage N2 (Table 1). These results indicated that *TRIM28* expression had more significant prognostic value in LUAD patients than in lung squamous cell carcinoma patients, and had more significant prognostic value in early-stage than in late-stage LUAD patients.

### ***TRIM28* expression is associated with the immune infiltration level**

Numerous studies have demonstrated that the immune infiltrates in various human tumor types are associated with the prognosis and response to therapy [9, 10, 43]. We used the TISIDB and Tumor Immune Estimation Resource (TIMER) databases to assess whether *TRIM28* expression was associated with the level of immune infiltration across human tumors. *TRIM28* levels correlated negatively with the levels of 28 types of tumor-infiltrating lymphocytes across human tumors in the TISIDB database (Figure 6A). *TRIM28* levels also correlated negatively with the levels of central memory CD8+ T cells ( $R = -0.212$ ,  $p < 0.001$ ), macrophages ( $R = -0.353$ ,  $p < 0.001$ ), natural killer T cells ( $R = -0.313$ ;  $p < 0.001$ ), myeloid-derived suppressor cells ( $R = -0.3$ ,  $p < 0.001$ ), regulatory T cells ( $R = -0.323$ ,  $p < 0.001$ ) and neutrophils ( $R = -0.287$ ,  $p < 0.001$ ) (Figure 6B). We then analyzed the relationship between *TRIM28* expression and immune infiltration in 39 tumor types in the TIMER database. *TRIM28* levels had strong negative associations with the infiltrating levels of CD8+ T cells in 24 tumor types, CD4+ T cells in 14 tumor types, macrophages in 25 tumor types,

neutrophils in 27 tumor types and dendritic cells in 24 tumor types. In LUAD samples, *TRIM28* levels correlated negatively with the infiltrating levels of B cells ( $R = -0.141$ ,  $p = 1.89e-03$ ), CD8+ T cells ( $R = -0.234$ ,  $p = 1.67e-07$ ), macrophages ( $R = -0.277$ ,  $p = 5.75e-10$ ), neutrophils ( $R = -0.192$ ,  $p = 2.16e-05$ ) and dendritic cells ( $R = -0.296$ ,  $p = 2.67e-11$ ) (Figure 6C). These results strongly suggested that *TRIM28* inhibits immune infiltration in LUAD.

We then explored the effects of *TRIM28* levels, clinicopathological characteristics and immune infiltration levels on survival using a multivariate Cox proportional hazards model. We found that age ( $p = 0.028$ ), stage ( $p < 0.001$ ), infiltrating B cell levels ( $p = 0.014$ ) and *TRIM28* levels ( $p < 0.001$ ) were independent predictors of survival in LUAD. However, only age ( $p = 0.024$ ) and stage 3 ( $p = 0.011$ ) were independent predictors of survival in lung squamous cell carcinoma (Table 2).

### **Analysis of genes co-expressed with *TRIM28* in LUAD**

Next, we used LinkedOmics [44] to identify genes that were co-expressed with *TRIM28* based on mRNA sequencing data from LUAD patients in TCGA. We generated a volcano map of all the genes associated with *TRIM28*, and found that interferon regulatory factor 5 (*IRF5*) and *IRF8* levels correlated negatively with *TRIM28* levels (Figure 7A). We also downloaded two mRNA expression datasets (GSE43580 and GSE7670) from the Gene Expression Omnibus (GEO) [34, 45]. We divided the samples in each dataset into two groups according to *TRIM28* expression, and we analyzed the DEGs between patients with higher and lower *TRIM28* levels. The volcano graphs in Figures 7B and 7C display the DEGs in GSE43580 and GSE7670, respectively. We then used a Venn diagram to evaluate the overlapping DEGs from Figure 7A–7C (Figure 7D). There were 429 common DEGs, including *IRF5*, *IRF8*, *B2M*, *CD44*, *HLA-DRA*, *HLA-DRB1* and *HLA-E*.

We then performed GO and KEGG analyses of these DEGs using Metascape [32]. We identified the top 14 GO enrichment terms (Figure 7E), which included the regulation of cytokine production and the interferon-gamma signaling pathway. The top 13 KEGG enrichment terms (Figure 7F) included the Toll-like receptor signaling pathway and ubiquitin-induced proteolysis. The correlations among the top 10 enriched terms from the GO analysis are shown as a network in Figure 7G. We also performed a Gene Set Enrichment Analysis using TCGA data, and found that the interferon-gamma and Toll-like receptor signaling pathways were enriched (Figure 7H). Combined with



**Table 1. Correlation between TRIM28 mRNA expression and prognosis in lung cancer patients with different clinicopathological characteristics, determined via Kaplan-Meier plotter.**

Clinicopathological characteristics	OS (n = 1928)			FP (n = 646)		
	N	Hazard ratio	P-value	N	Hazard ratio	P-value
Sex						
Female	715	2.11(1.54-2.9)	<0.001	468	2.09(1.57-2.78)	<0.001
male	1387	1.48(1.25-1.75)	<0.001	514	1.87(1.44-2.44)	<0.001
Histology						
Adenocarcinoma	720	2.65(1.96-3.59)	<0.001	461	2.00(1.45-2.75)	<0.001
Squamous cell carcinoma	524	1.25(0.96-1.64)	0.095	141	2.15(1.27-3.64)	0.003
Grade						
I	201	0.81(0.56-1.16)	0.250	140	0.81(0.51-1.29)	0.380
II	310	1.34(0.96-1.87)	0.079	165	1.68(1.08-2.62)	0.020
III	77	0.64(0.28-1.47)	0.290	51	1.36(0.6-3.05)	0.460
Stage						
1	577	2.45(1.85-3.25)	<0.001	325	1.47(0.94-2.31)	0.091
2	244	2.2(1.45-3.35)	<0.001	130	0.79(0.46-1.35)	0.380
3	70	0.69(0.39-1.21)	0.200	19	-	-
4	4	-	-	0	-	-
Stage T						
1	437	1.37(0.97-1.92)	0.070	177	2.31(1.38-3.89)	0.001
2	589	1.26(0.99-1.6)	0.056	351	1.45(1.08-1.96)	0.014
3	81	0.8(0.47-1.34)	0.390	21	0.58(0.21-1.62)	0.290
4	46	1.46(0.72-2.96)	0.290	7	-	-
Stage N						
0	781	1.31(1.05-1.64)	0.015	374	1.83(1.3-2.56)	<0.001
1	252	1.29(0.94-1.76)	0.110	130	1.96(1.24-3.1)	0.004
2	111	1.18(0.78-1.78)	0.430	51	1.82(0.91-3.65)	0.087
Stage M						
0	681	1.61(1.3-1.99)	<0.001	195	1.56(0.94-2.59)	0.080
1	10	-	-	0	-	-
Smoking history						
Never smoked	205	4.1(2.17-7.73)	<0.001	193	2.72(1.66-4.45)	<0.001
Smoked	820	1.87(1.39-2.52)	<0.001	603	1.71(1.34-2.18)	<0.001

OS, overall survival; FP, first progression.

our previous results, these results may indicate that TRIM28 inhibits the interferon-gamma and Toll-like receptor signaling pathways by increasing the ubiquitination (degradation) of IRF5 and IRF8, ultimately suppressing immune infiltration.

### TRIM28 may worsen the TIME by increasing the SUMOylation of IRF5 and IRF8

To identify potential SUMO substrates of TRIM28, we queried TRIM28 as E3 in the web tool of UbiBrowser [46]. The 79 predicted substrates with middle-confidence interactions and 347 predicted substrates with low-confidence interactions are presented in Supplementary Table 4. Figure 8A displays some of the substrates, and Figure 8B displays the predicted binding regions of IRF5 and IRF8 to TRIM28. We then performed a correlation analysis, which indicated that TRIM28 expression correlated negatively with IRF5 and

IRF8 expression in TCGA ( $R = -0.210$ ,  $p < 0.001$ ;  $R = -0.302$ ,  $p < 0.001$ ; Figure 8C and 8D), GSE43580 ( $R = -0.371$ ,  $p < 0.001$ ;  $R = -0.420$ ,  $p < 0.001$ ; Figure 8E and 8F) and GSE7670 ( $R = -0.491$ ,  $p = 0.004$ ;  $R = -0.430$ ,  $p = 0.014$ ; Figure 8G and 8H), respectively. Moreover, TRIM28 expression exhibited a strong negative correlation with stromal scores and immune scores (Figure 8I and 8J), while IRF5 and IRF8 expression exhibited strong positive correlations with stromal scores (Figure 8K and 8M) and immune scores (Figure 8L and 8N), respectively.

To verify our hypothesis that TRIM28 downregulates IRF5 and IRF8, we knocked down TRIM28 in two different LUAD cell lines (PC9 and H1299). The knockdown efficiency was validated through Western blotting (Figure 8O). As expected, IRF5 and IRF8 levels increased significantly when TRIM28 was knocked down (Figure 8O).

## DISCUSSION

Despite the latest advances in molecular targeted therapy and immunotherapy for LUAD, local and distant failures remain major therapeutic issues. In addition, immunotherapy is only effective in 20-30% of patients, and our knowledge of the TIME is inadequate. Therefore, we performed a comprehensive bioinformatics analysis to identify genes that may alter the TIME and prognosis of LUAD patients. We found that *TRIM28* levels correlated negatively with the stromal scores, immune scores and immune cell infiltration levels of LUAD patients. *TRIM28* was previously reported as a cofactor that regulates the activity of various immune-related cells and the expression of multiple cytokines [17–25]. Our

functional analyses of *TRIM28* supported these conclusions.

Most of the published data suggest that *TRIM28* exerts oncogenic effects, and microarray analyses in a wide variety of tumors have revealed that *TRIM28* mRNA levels are significantly greater in tumor tissues than in normal tissues [35, 36]. Our study also demonstrated that *TRIM28* mRNA levels were significantly greater in most tumor tissues than in adjacent healthy tissues, especially in the case of LUAD. However, we found some discrepancies in particular cancer types. For example, in breast cancer, three cohorts indicated that higher *TRIM28* levels were marginally associated with poorer DFS and DSS (Figure 5A–5C), but two other datasets demonstrated that lower *TRIM28* levels were

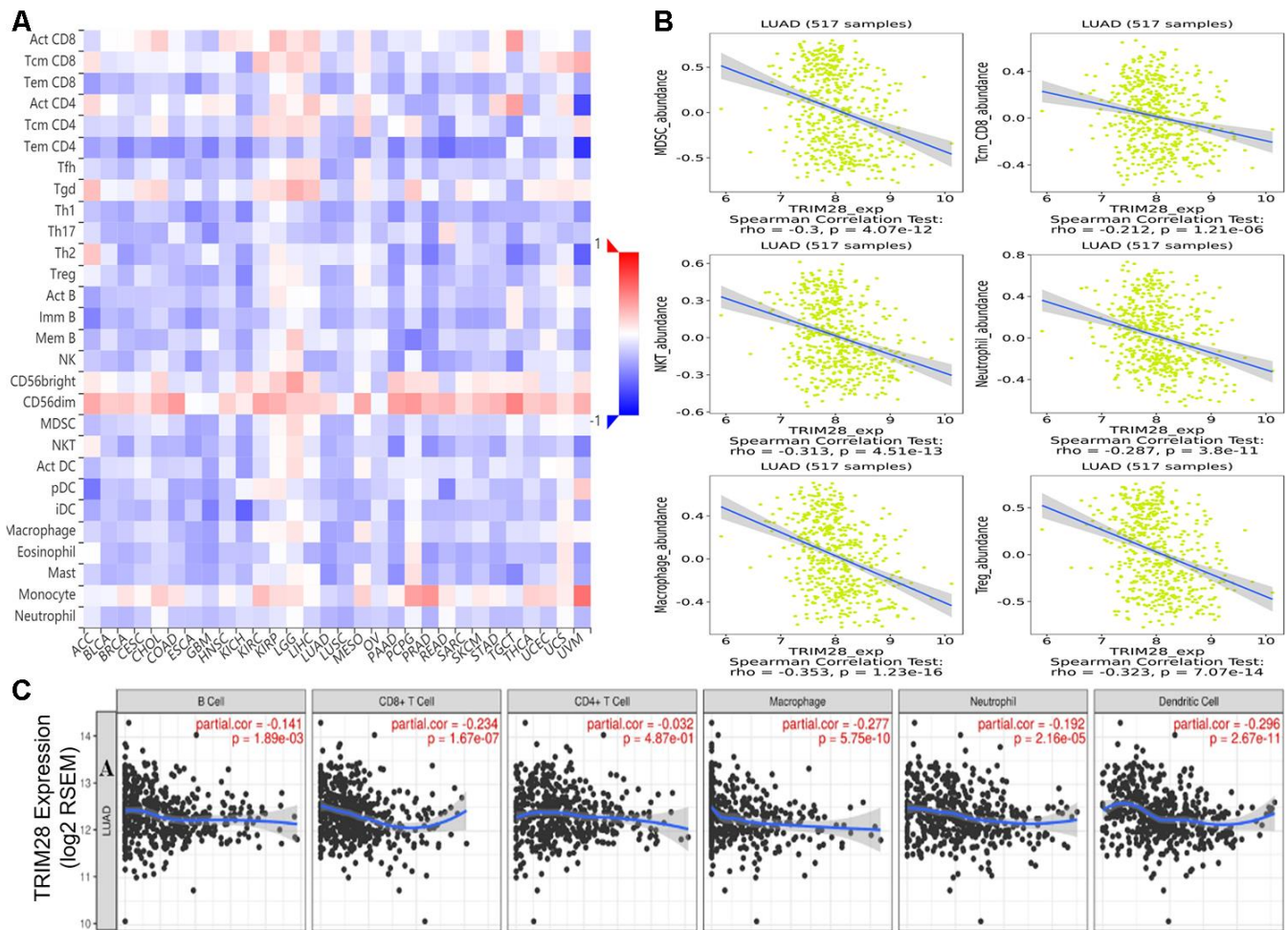


**Figure 6. Correlation of TRIM28 expression with immune cell infiltration.** (A) TRIM28 levels were significantly negatively associated with the levels of most tumor-infiltrating lymphocytes across human tumors in the TISIDB database. (B) TRIM28 levels correlated negatively with the levels of central memory CD8+ T cells, myeloid-derived suppressor cells, natural killer T cells, macrophages, neutrophils and regulatory T cells. (C) TRIM28 levels correlated negatively with the infiltrating levels of B cells, CD8+ T cells, macrophages, neutrophils and dendritic cells in LUAD in the TIMER database. LUAD, lung adenocarcinoma; Tcm\_CD8, Central memory CD8 T cell; MDSC, Myeloid-derived suppressor cell; NKT, Natural killer T cell; Treg, regulatory T cell. TILs, tumor-infiltrating lymphocytes.

**Table 2. A multivariate Cox proportional hazards model was used to explore the effects of TRIM28 expression, clinicopathological characteristics and immune infiltration levels on survival.**

LUAD (N=436)	Variable	Coef	HR	95%CI_l	95%CI_u	P-value
	Age	0.019	1.019	1.002	1.037	0.028
	Gender	-0.258	0.772	0.553	1.079	0.130
	Stage2	0.857	2.356	1.550	3.583	<0.001
	Stage3	1.065	2.901	1.900	4.430	<0.001
	Stage4	1.256	3.510	1.918	6.424	<0.001
	Purity	0.357	1.430	0.628	3.257	0.395
	B cell	-3.507	0.030	0.002	0.493	0.014
	CD8+Tcell	0.471	1.601	0.217	11.801	0.644
	CD4+Tcell	2.090	8.086	0.537	121.759	0.131
	Macrophage	0.782	2.187	0.138	34.629	0.579
	Neutrophil	-1.888	0.151	0.003	7.376	0.341
	Dendritic	0.219	1.245	0.297	5.208	0.765
	TRIM28	0.595	1.813	1.317	2.495	<0.001
LUSC (N=452)		Coef	HR	95%CI_l	95%CI_u	P-value
	Age	0.02	1.02	1.003	1.038	0.024
	Gender	0.303	1.353	0.957	1.913	0.087
	Stage2	0.107	1.113	0.792	1.564	0.539
	Stage3	0.495	1.641	1.121	2.402	0.011
	Stage4	0.982	2.67	0.949	7.507	0.063
	Purity	-0.128	0.88	0.422	1.834	0.733
	B cell	1.298	3.663	0.298	45.061	0.311
	CD8+Tcell	-1.727	0.178	0.028	1.124	0.066
	CD4+Tcell	0.705	2.023	0.153	26.753	0.593
	Macrophage	-0.339	0.713	0.061	8.326	0.787
	Neutrophil	0.980	2.665	0.099	71.525	0.559
	Dendritic	0.722	2.059	0.489	8.662	0.325
	TRIM28	0.000	1.000	0.774	1.292	1.000

Coef, regression coefficient; HR, hazard ratio; 95%CI\_l, 95% confidence interval lower limit; 95%CI\_u, 95% confidence interval upper limit.

associated with poorer DMFS and OS in the PrognScan database (Figure 5D and 5E). In addition, *TRIM28* expression had little impact on breast cancer prognosis in the Kaplan-Meier plotter (Supplementary Figure 1) and no effect on breast cancer prognosis in GEPIA. These discrepancies may reflect differing data collection approaches or underlying mechanisms. However, in all the databases we examined, higher *TRIM28* expression was associated with a poorer prognosis of LUAD. These findings strongly suggested that *TRIM28* is a prognostic biomarker in LUAD.

The immune system is a critical regulator of tumor biology and has the capacity to support or inhibit tumor development, growth, invasion and metastasis. Tumor cells adopt a variety of mechanisms to avoid immune recognition and destruction, including: 1) downregulating human leukocyte antigen (HLA) class I molecules such as HLA-A, HLA-B, HLA-C and B2M on the cancer cell surface; 2) altering the antigen-presenting cell number or function; 3) lacking costimulation molecules such as B7-1, B7-2 and CD40; 4) promoting negative immune

regulation by regulatory T cells and mesenchymal stem cells; 5) secreting immunosuppressive cytokines such as interleukin (IL)-10, transforming growth factor  $\beta$  and IL-6; 6) aberrantly expressing apoptosis-related molecules such as Fas, Fas ligand, tumor necrosis factor-related apoptosis inducing ligand and BAX; and 7) inhibiting effector cells via inhibitory ligands such as PD-L1, cytotoxic T-lymphocyte associated protein 4 and lymphocyte activation gene 3 [47–52]. The types and frequencies of these immune escape mechanisms vary among different cancer types. The proportions and activities of effector cells and antigen-presenting cells such as dendritic cells, B cells and macrophages are often reduced in the peripheral blood of cancer patients, while the numbers of immune-suppressive mesenchymal stem cells, natural killer T cells and regulatory T cells are generally elevated [49, 50]. Using different bioinformatics methods, we demonstrated that *TRIM28* expression correlated negatively with the immune infiltration of LUAD. Thus, we proposed that *TRIM28* may negatively regulate the TIME and thereby promote tumor development and progression.

There are several possible mechanisms by which TRIM28 could impair immune cell infiltration. 1) TRIM28 critically inhibits the induction of Foxp3, the number of regulatory T cells, Th17 cells differentiation [20, 53, 54], and macrophage activation [18, 24],

suggesting that TRIM28 may impair the TIME. 2) TRIM28 inhibits the effects of IRF5 on gene expression, and IRF5 has been reported to repress anti-inflammatory genes such as *IL-10* [18]. 3) TRIM28 negatively regulates IRF7, which is a potent transcription

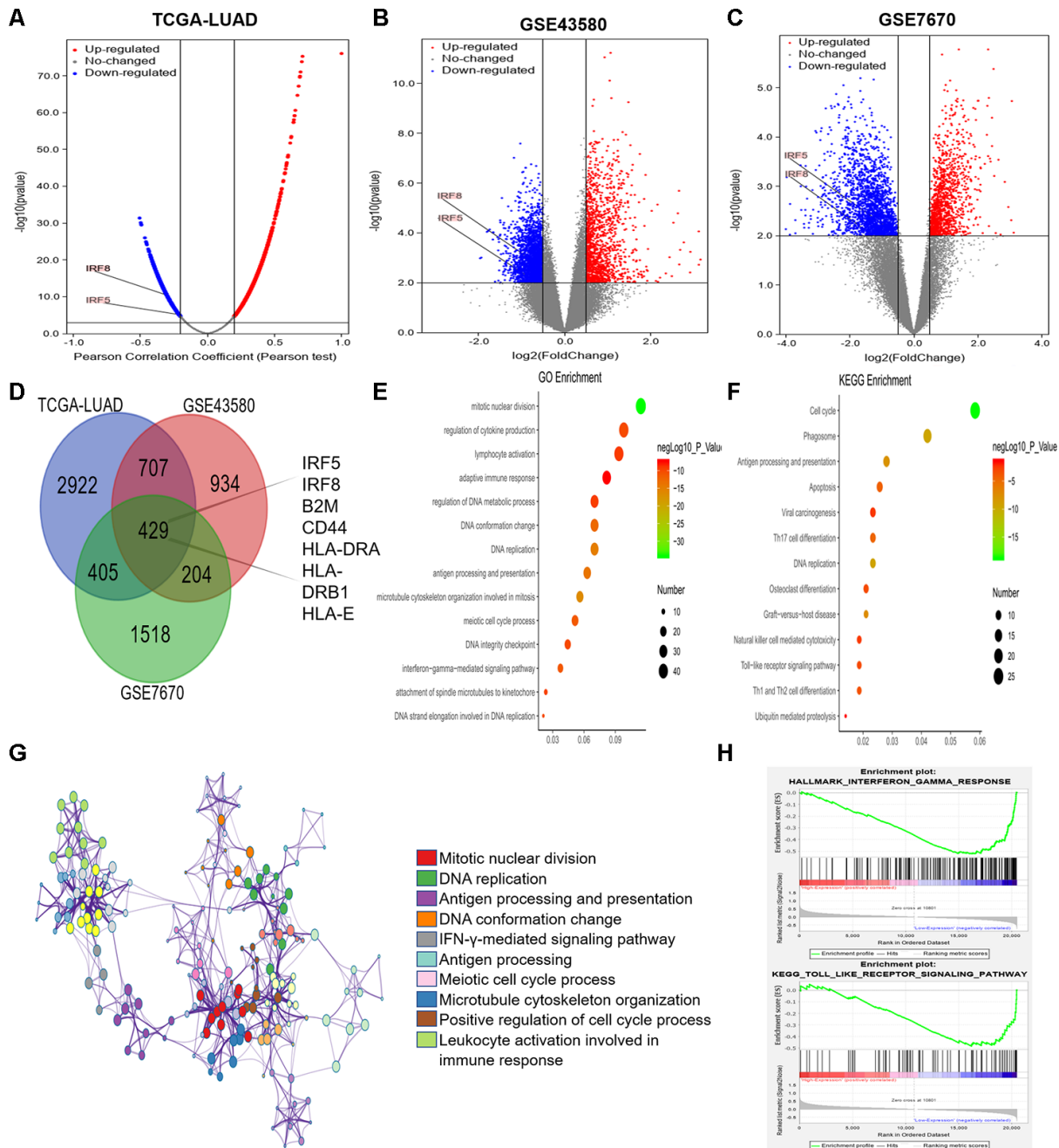


**Figure 7. Analysis of DEGs according to TRIM28 expression in LUAD patients.** (A) Volcano map showing all the genes associated with TRIM28 in LUAD. (B, C) Volcano maps showing all the DEGs based on TRIM28 expression. (D) Venn diagram showing the number of common DEGs. (E, F) Top 14 GO enrichment terms (E) and top 13 KEGG enrichment terms (F) for all DEGs, analyzed in Metascape. (G) Associations among the top 10 cluster enrichment terms analyzed by Metascape, displayed as a network. An edge links terms with a similarity score > 0.3. (H) Gene Set Enrichment Analysis according to the expression of TRIM28 in TCGA. GO, gene ontology; DEGs, differentially expressed genes; LUAD, lung adenocarcinoma; GSEA, Gene Set Enrichment Analysis; TCGA, The Cancer Genome Atlas; GSE, Gene Expression Omnibus data series.

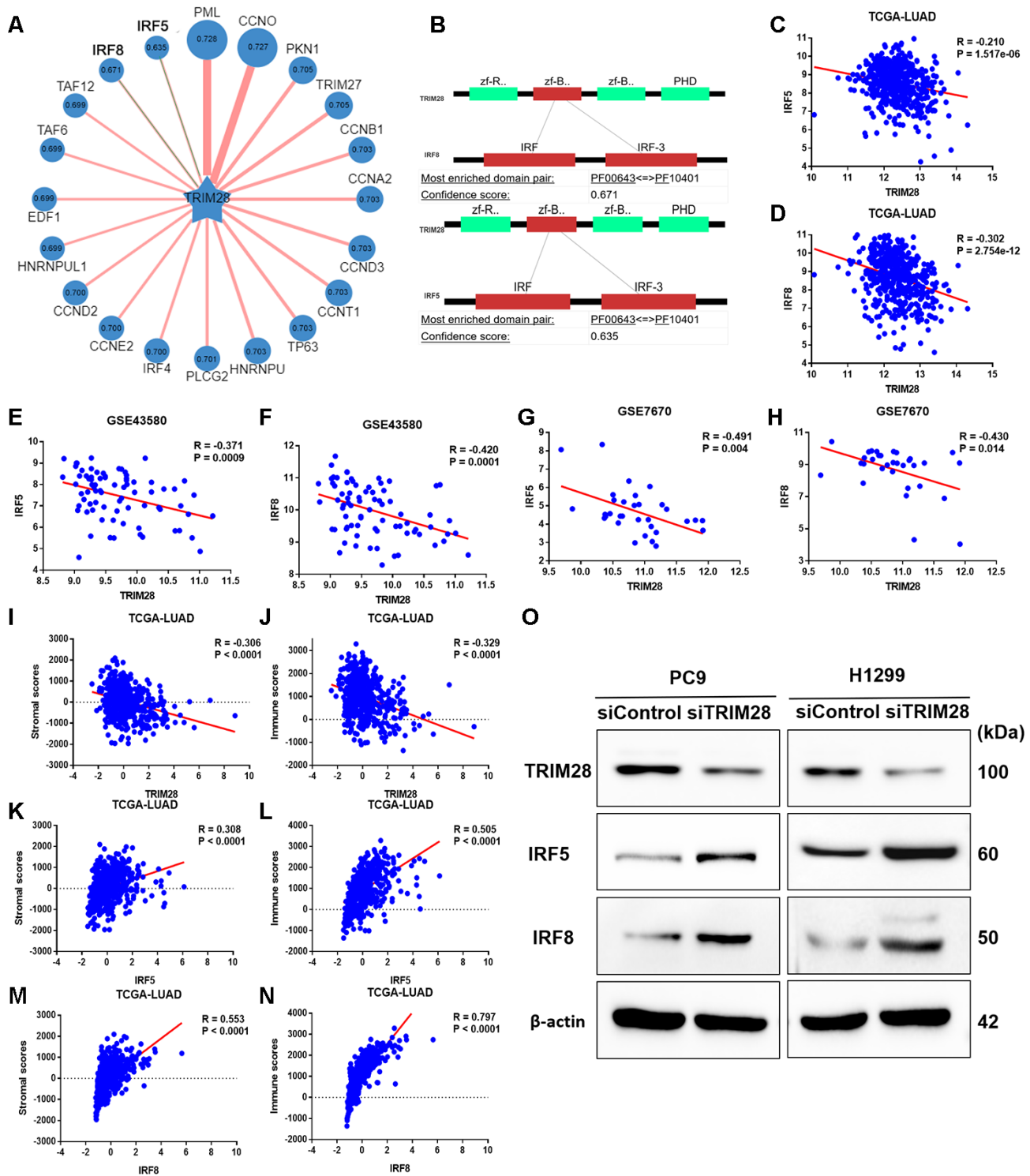


**Figure 8. The association of TRIM28 with IRF5 and IRF8.** (A) Network view of predicted E3-substrate interactions in UbiBrowser web services. In network view, the central node is the queried E3 ligase, and the surrounding nodes are the predicted substrates. The width of the edge reflects the confidence of the interaction. (B) The possible binding regions of IRF5 and IRF8 to TRIM28. (C–H) TRIM28 expression exhibited a significant negative correlation with IRF5 and IRF8 expression in TCGA (C, D), GSE43580 (E, F) and GSE7670 (G, H). (I–N) TRIM28 expression exhibited a strong negative correlation with stromal scores (I) and immune scores (J), while IRF5 and IRF8 levels exhibited strong positive relationships with stromal scores (K, M) and immune scores (L, N), respectively. (O) The expression of IRF5 and IRF8 after knocking down TRIM28 in two different LUAD cell lines (PC9 and H1299) through Western blotting. The gels have been run under the same experimental conditions. The blot of IRF5 in H1299 is obtained from the combined image merging the blot image and the ladder image. LUAD, lung adenocarcinoma; TCGA, The Cancer Genome Atlas; GSE, Gene Expression Omnibus data series.

factor of type I interferons and interferon-stimulated genes and is known as the master regulator of type I interferon-dependent immune responses [22]. 4) TRIM28 suppressed TNF- $\alpha$ -induced IL-6 production and transcriptional activation of NF- $\kappa$ B [24, 25]. 5) TRIM28 functions as an important negative regulator of the expression of IFN- $\beta$ , IFN- $\gamma$ , IL-6 and IL-8 during viral infection [55]. We found that TRIM28 may inhibit the interferon-gamma and Toll-like receptor signaling pathways by increasing the SUMOylation of IRF5 and IRF8, ultimately suppressing immune infiltration in LUAD. We confirmed these findings by performing a correlation analysis and validations in LUAD cell lines. Overall, TRIM28 appears to globally manage various immune-related cells and to reduce immune infiltration by altering the expression of diverse chemokines and molecular signaling pathways.

Using a multivariate Cox proportional hazards model, we confirmed that *TRIM28* expression and infiltrating B cell levels were independent predictors of survival in LUAD. Tumor-infiltrating B cell levels are strongly associated with the prognosis of various tumor types [56–59]. The mechanisms by which tumor-infiltrating B cells influence tumor immunity may include: 1) functioning as antigen-presenting cells to facilitate innate cellular immunity in the TIME; 2) activating CD8<sup>+</sup> T cells to promote antigen-specific antitumor immune responses [60]; and 3) promoting adaptive immunity by inducing the release of circulating cytokines to recruit immunosuppressive cells [61]. However, further study is needed to understand their functions and mechanisms.

The PD1/PD-L1 cascade is a highly effective therapeutic target in immunotherapy [4–7]. PD-L1 is expressed in a variety of cancer types in either a constitutive (or intrinsic) or interferon-induced manner. The results of our research and previous studies suggest that TRIM28 regulates interferons in multiple ways. Liang et al. [62] reported that verteporfin, a small-molecule inhibitor, inhibited PD-L1 by inducing autophagy and disrupting the STAT1-IRF1-TRIM28 signaling axis, thus exerting antitumor effects in immunotherapy. However, the efficacy of immunotherapy depends not only on immune infiltration and PD-L1 expression, but also on the tumor mutation burden, epidermal growth factor receptor mutation status and other unknown factors [63]. Thus, further research is needed to evaluate the potential of TRIM28 as a therapeutic target in immunotherapy.

There are several limitations to our research. First, this was a retrospective analysis based on public databases (TCGA and GEO). The number of included patients was limited, and it was difficult to account for variations in

race, age and geographic area. Thus, additional *in vivo* and *in vitro* experiments are required for functional and clinical verification. Second, considering the possible spatial and temporal heterogeneity of the TIME, immune and stromal assessments should ideally be performed at the core and infiltrating edges of the tumor, respectively. However, all the data in this study were from samples in the core area of the tumor.

In conclusion, the present study demonstrated that TRIM28 worsens the TIME and is highly expressed in LUAD. Increased *TRIM28* expression was associated with reduced levels of various infiltrating immune cells, and was an independent prognostic factor in LUAD. TRIM28 may negatively regulate the TIME by increasing the SUMOylation of IRF5 and IRF8. Thus, our research has provided new insights into the suppressive function of TRIM28 in the TIME and the potential of *TRIM28* as a prognostic biomarker in LUAD.

## MATERIALS AND METHODS

### Gene expression profile data

TCGA data containing RNA sequencing results and clinical information (level 3 data) were downloaded from the cBioPortal database (<http://www.cbioportal.org>). The *TRIM28* expression data from GSE32863 [33], GSE7670 [34], GSE19188 [35] and the Beer Lund dataset [36] were downloaded from Oncomine (<https://www.oncomine.org/resource/main.html>) [64]. Two mRNA expression datasets (GSE43580 and GSE7670) were downloaded from the GEO database (<https://www.ncbi.nlm.nih.gov/geo/>) [34, 45], and were based on the GPL570 (Affymetrix Human Genome U133 Plus 2.0 Array) and GPL96 (Affymetrix Human Genome U133A Array) platforms, respectively. The GSE43580 dataset included 77 LUAD patients, while the GSE7670 dataset included 28 LUAD patients.

### DEG identification

R software (version 3.6.1) was used for detailed analyses in this study. We used the LinkedOmics database (<http://www.linkedomics.org/login.php>) [44] to analyze the genes co-expressed with *TRIM28* in LUAD. All DEG analyses were performed using the "limma" R package. Fold-changes in gene expression were calculated with threshold criteria of a  $|\log_2\text{fold-change}| > 0.5$ , false discovery rate  $< 0.05$  and adjusted  $p < 0.001$  for DEG selection.

### Functional enrichment analysis of DEGs

To explore the functions of the overlapping DEGs, we performed GO and KEGG analyses in Metascape

(<http://metascape.org/gp>) [32]. The selected GO terms were from the "Biological Process" annotation datasets. The cutoff value for pathway screening was set to  $p < 0.01$ . The levels of significant DEGs were visualized on a heatmap based on hierarchical clustering analyses using the average linkage method.

### PPI network construction and analysis

STRING (Version 11.0, <http://string-db.org>) is a database of known and predicted PPI networks. We used this tool to construct PPI networks and predict potential interactions between candidate genes. Interactions were considered significant above a cutoff score of 0.4. In addition, Cytoscape software (Version 3.7.2, <http://www.cytoscape.org/>) [65] and the cytoHubba plugin [66] were used to explore the hub genes in the PPI network. Eleven methods can be used to explore essential nodes in PPI networks, but maximal clique centrality performs better than the others.

### RNA and protein expression analyses

OncoPrint [64] was used to explore the *TRIM28* levels in different tumor types. The parameters were adjusted according to the following criteria:  $p$ -value of  $1e-4$ , fold change of 2 and gene ranking in the top 10%.

TIMER (<https://cistrome.shinyapps.io/timer/>) [67] is a comprehensive database that can be used to estimate the abundance of immune infiltrates and characterize the tumor-immune interactions across diverse tumor types. The levels of six tumor-infiltrating immune subsets, including B cells, CD4+ T cells, CD8+ T cells, neutrophils, macrophages and dendritic cells, are precalculated for 10,897 tumors from TCGA. We used TIMER to explore *TRIM28* expression in various tumor types.

In addition, the UALCAN database [68] can be used to analyze protein expression based on data from the Clinical Proteomic Tumor Analysis Consortium Confirmatory/Discovery dataset. We evaluated the protein levels of *TRIM28* in various cancers by performing a Clinical Proteomic Tumor Analysis Consortium analysis.

### Prognosis analysis

The PrognScan database (<http://www.abren.net/PrognScan/>) was used to determine the relationship between *TRIM28* levels and the prognoses of different tumor types [69]. PrognScan analyzes the correlations between gene levels and prognostic indicators such as DFS and OS using a large number of public tumor

microarray datasets. The threshold was set to a Cox  $p$ -value of 0.05.

Kaplan-Meier plotter (<http://kmplot.com/analysis/>) [70], an online database of published microarray datasets, can be used to assess the impact of 54,675 genes on survival using 18,674 cancer samples, including samples from 5,143 breast, 1,816 ovarian, 2,437 lung and 1,065 gastric cancer patients. We used the Kaplan-Meier plotter to explore the relationship between *TRIM28* expression and prognosis in breast, lung, ovarian and gastric cancers. The HR, 95% CI and  $p$ -value were all calculated.

GEPIA (<http://gepia.cancer-pku.cn/index.html>) [71] is an online database that can be used for differential gene expression analysis, profile plotting, correlation analysis, patient survival analysis, similar gene detection and dimensionality reduction analysis based on TCGA and Genotype-Tissue Expression data. We used GEPIA to analyze the prognostic value of *TRIM28* expression based on the log-rank test in 33 cancer types.

### Stromal and immune score calculation and immune infiltration analysis

Using the "Estimate" R package, we calculated the stromal and immune scores of LUAD patients based on their gene expression profiles [11]. To verify the relationships between the target genes and the TIME, we used the TIMER database and another comprehensive database (TISIDB, <http://cis.hku.hk/TISIDB/index.php>) [72]. TISIDB integrates multiple heterogeneous data types. Spearman correlations between *TRIM28* levels and tumor-infiltrating lymphocyte levels across human cancers were analyzed. All hypothetical tests were two-sided, and  $p$ -values  $< 0.05$  were considered significant.

### Query for E3-TRIM28 interactions in UbiBrowser

UbiBrowser (<http://ubibrowser.ncpsb.org/>) [46] is an integrated bioinformatics platform that can be used to predict proteome-wide human E3-substrate networks based on naïve Bayesian networks. It currently contains 1,295 literature-reported E3-substrate interactions and 8,255 predicted E3-substrate interactions. We used it to predict the potential substrates of *TRIM28*.

### Cell culture and transfection

We obtained the PC9 cell line from the RIKEN BioResource Center (Tsukuba, Japan), and purchased the H1299 cell line from the American Type Culture Collection (Manassas, VA, USA). The cells were propagated in RPMI 1640 medium (Invitrogen,

Carlsbad, CA, USA) supplemented with 10 % fetal bovine serum and antibiotics.

For transfection, the cells ( $1 \times 10^5$ ) were seeded in six-well plates. The cells were transfected using jetPRIME reagent (Polyplus transfection) with 110 pmol of ON-TARGETplus SMARTpool-Human TRIM28 (L-005046-00-0020, Dharmacon) according to the manufacturers' protocols.

### Western blotting

The Western blot assay was conducted as previously described. Briefly, the cells were washed in cold  $1 \times$  phosphate-buffered saline and lysed in ice-cold radioimmunoprecipitation assay buffer supplemented with protease inhibitors on ice for 30 min. The protein concentrations were quantified using the bicinchoninic acid method according to the manufacturer's instructions. The protein samples were subjected to sodium dodecyl sulfate-polyacrylamide gel electrophoresis and then transferred to nitrocellulose membranes (BioRad, USA). The membranes were blocked with 5% non-fat milk for one hour, and then incubated overnight with primary antibodies diluted in 2% bovine serum albumin. After being washed, the membranes were incubated with horseradish peroxidase-conjugated secondary antibodies for one hour. The primary antibodies used for immunodetection were rabbit monoclonal anti-TRIM28 (#4124, Cell Signaling Technology, USA), rabbit polyclonal anti-IRF5 (#20261, Cell Signaling Technology), rabbit monoclonal anti-IRF8 (#5628, Cell Signaling Technology) and rabbit polyclonal anti- $\beta$ -actin (#ab8227, Abcam, UK). The secondary antibody was obtained from Abcam (#ab205718). Blots were visualized with an enhanced chemiluminescence reagent (Supersignal; Pierce, Rockford, IL, USA).

### Statistical analysis

The results from the OncoPrint database are displayed with *p*-values, fold-changes and ranks. Interactive heatmaps were constructed using Next-Generation Clustered Heatmaps [73]. PrognScan, GEPIA and Kaplan-Meier plots were used to create survival curves, and the results are displayed with HRs and *p*-values or Cox *p*-values. A multivariate Cox proportional hazards model was used to analyze the independent prognostic factors for lung cancer. *P*-values  $< 0.05$  were considered statistically significant.

### Abbreviations

ACC: adrenocortical carcinoma; BLCA: bladder urothelial carcinoma; BRCA: breast invasive carcinoma;

CI: confidence interval; DEGs: differentially expressed genes; DFS: disease-free survival; DMFS: distant metastasis-free survival; DSS: disease-specific survival; FP: first progression; HR: hazard ratio; KIRP: kidney renal papillary cell carcinoma; LGG: brain lower-grade glioma; LUAD: lung adenocarcinoma; LUSC: lung squamous cell carcinoma; MESO: mesothelioma; NSCLC: non-small-cell lung cancer; OS: overall survival; PD1: programmed cell death-1; PD-L1: programmed cell death ligand-1; PPI: protein-protein interaction; RFS: recurrence-free survival; SKCM: skin cutaneous melanoma; TCGA: The Cancer Genome Atlas; TIME: tumor immune microenvironment; TRIM: Tripartite motif-containing.

### AUTHOR CONTRIBUTIONS

J.L. and X.H. conceived and designed the experiments; X.H., L.J.C. and J.L. performed the experiments; J.L., X.Q.M., H.J.W. and X.F.H. analyzed the data; H.B.W., W.J.L. and J.L. prepared the figures and tables; J.L., D.H. and Y.Q.Z. drafted the work or revised it critically for important content. All authors reviewed the manuscript.

### CONFLICTS OF INTEREST

The authors report no conflicts of interest.

### FUNDING

This study was supported by Grants-in-Aid from the Medical Innovation Talent Program, Health Department of Henan Province, China (Project No. 201702247).

### REFERENCES

1. Torre LA, Bray F, Siegel RL, Ferlay J, Lortet-Tieulent J, Jemal A. Global cancer statistics, 2012. *CA Cancer J Clin.* 2015; 65:87–108. <https://doi.org/10.3322/caac.21262> PMID:[25651787](https://pubmed.ncbi.nlm.nih.gov/25651787/)
2. Jie-Liu, Li XY, Zhao YQ, Liu RQ, Zhang JB, Ma J, Chen LJ, Hu XF. Genotype-phenotype correlation in Chinese patients with pulmonary mixed type adenocarcinoma: relationship between histologic subtypes, TITF-1/SP-a expressions and EGFR mutations. *Pathol Res Pract.* 2014; 210:176–81. <https://doi.org/10.1016/j.prp.2013.11.013> PMID:[24370340](https://pubmed.ncbi.nlm.nih.gov/24370340/)
3. Hanahan D, Weinberg RA. Hallmarks of cancer: the next generation. *Cell.* 2011; 144:646–74. <https://doi.org/10.1016/j.cell.2011.02.013> PMID:[21376230](https://pubmed.ncbi.nlm.nih.gov/21376230/)



4. Rittmeyer A, Barlesi F, Waterkamp D, Park K, Ciardiello F, von Pawel J, Gadgeel SM, Hida T, Kowalski DM, Dols MC, Cortinovis DL, Leach J, Polikoff J, et al, and OAK Study Group. Atezolizumab versus docetaxel in patients with previously treated non-small-cell lung cancer (OAK): a phase 3, open-label, multicentre randomised controlled trial. *Lancet*. 2017; 389:255–65. [https://doi.org/10.1016/S0140-6736\(16\)32517-X](https://doi.org/10.1016/S0140-6736(16)32517-X) PMID:27979383
5. Herbst RS, Baas P, Kim DW, Felip E, Perez-Gracia JL, Han JY, Molina J, Kim JH, Arvis CD, Ahn MJ, Majem M, Fidler MJ, de Castro G Jr, et al. Pembrolizumab versus docetaxel for previously treated, PD-L1-positive, advanced non-small-cell lung cancer (KEYNOTE-010): a randomised controlled trial. *Lancet*. 2016; 387:1540–50. [https://doi.org/10.1016/S0140-6736\(15\)01281-7](https://doi.org/10.1016/S0140-6736(15)01281-7) PMID:26712084
6. Brahmer J, Reckamp KL, Baas P, Crinò L, Eberhardt WE, Poddubskaya E, Antonia S, Pluzanski A, Vokes EE, Holgado E, Waterhouse D, Ready N, Gainor J, et al. Nivolumab versus docetaxel in advanced squamous-cell non-small-cell lung cancer. *N Engl J Med*. 2015; 373:123–35. <https://doi.org/10.1056/NEJMoa1504627> PMID:26028407
7. Borghaei H, Paz-Ares L, Horn L, Spigel DR, Steins M, Ready NE, Chow LQ, Vokes EE, Felip E, Holgado E, Barlesi F, Kohlhäufel M, Arrieta O, et al. Nivolumab versus docetaxel in advanced nonsquamous non-small-cell lung cancer. *N Engl J Med*. 2015; 373:1627–39. <https://doi.org/10.1056/NEJMoa1507643> PMID:26412456
8. Ali A, Goffin JR, Arnold A, Ellis PM. Survival of patients with non-small-cell lung cancer after a diagnosis of brain metastases. *Curr Oncol*. 2013; 20:e300–06. <https://doi.org/10.3747/co.20.1481> PMID:23904768
9. Waniczek D, Lorenc Z, Śnietura M, Wesecki M, Kopec A, Muc-Wierzoń M. Tumor-associated macrophages and regulatory T cells infiltration and the clinical outcome in colorectal cancer. *Arch Immunol Ther Exp (Warsz)*. 2017; 65:445–54. <https://doi.org/10.1007/s00005-017-0463-9> PMID:28343267
10. Zhang H, Liu H, Shen Z, Lin C, Wang X, Qin J, Qin X, Xu J, Sun Y. Tumor-infiltrating neutrophils is prognostic and predictive for postoperative adjuvant chemotherapy benefit in patients with gastric cancer. *Ann Surg*. 2018; 267:311–18. <https://doi.org/10.1097/SLA.0000000000002058> PMID:27763900
11. Yoshihara K, Shahmoradgoli M, Martínez E, Vegesna R, Kim H, Torres-Garcia W, Treviño V, Shen H, Laird PW, Levine DA, Carter SL, Getz G, Stemke-Hale K, et al. Inferring tumour purity and stromal and immune cell admixture from expression data. *Nat Commun*. 2013; 4:2612. <https://doi.org/10.1038/ncomms3612> PMID:24113773
12. Hao L, Leng J, Xiao R, Kingsley T, Li X, Tu Z, Yang X, Deng X, Xiong M, Xiong J, Zhang Q. Bioinformatics analysis of the prognostic value of Tripartite Motif 28 in breast cancer. *Oncol Lett*. 2017; 13:2670–78. <https://doi.org/10.3892/ol.2017.5764> PMID:28454449
13. Cheng B, Ren X, Kerppola TK. KAP1 represses differentiation-inducible genes in embryonic stem cells through cooperative binding with PRC1 and derepresses pluripotency-associated genes. *Mol Cell Biol*. 2014; 34:2075–91. <https://doi.org/10.1128/MCB.01729-13> PMID:24687849
14. Addison JB, Koontz C, Fugett JH, Creighton CJ, Chen D, Farrugia MK, Padon RR, Voronkova MA, McLaughlin SL, Livengood RH, Lin CC, Ruppert JM, Pugacheva EN, Ivanov AV. KAP1 promotes proliferation and metastatic progression of breast cancer cells. *Cancer Res*. 2015; 75:344–55. <https://doi.org/10.1158/0008-5472.CAN-14-1561> PMID:25421577
15. Jin X, Pan Y, Wang L, Zhang L, Ravichandran R, Potts PR, Jiang J, Wu H, Huang H. MAGE-TRIM28 complex promotes the warburg effect and hepatocellular carcinoma progression by targeting FBP1 for degradation. *Oncogenesis*. 2017; 6:e312. <https://doi.org/10.1038/oncsis.2017.21> PMID:28394358
16. Czerwińska P, Mazurek S, Wiznerowicz M. The complexity of TRIM28 contribution to cancer. *J Biomed Sci*. 2017; 24:63. <https://doi.org/10.1186/s12929-017-0374-4> PMID:28851455
17. Santoni de Sio FR, Barde I, Offner S, Kapopoulou A, Corsinotti A, Bojkowska K, Genolet R, Thomas JH, Luescher IF, Pinschewer D, Harris N, Trono D. KAP1 regulates gene networks controlling T-cell development and responsiveness. *FASEB J*. 2012; 26:4561–75. <https://doi.org/10.1096/fj.12-206177> PMID:22872677
18. Eames HL, Saliba DG, Krausgruber T, Lanfrancotti A, Ryzhakov G, Udalova IA. KAP1/TRIM28: an inhibitor of IRF5 function in inflammatory macrophages. *Immunobiology*. 2012; 217:1315–24. <https://doi.org/10.1016/j.imbio.2012.07.026> PMID:22995936
19. Zhou XF, Yu J, Chang M, Zhang M, Zhou D, Cammas F,

- Sun SC. TRIM28 mediates chromatin modifications at the TCR $\alpha$  enhancer and regulates the development of T and natural killer T cells. *Proc Natl Acad Sci USA*. 2012; 109:20083–88.  
<https://doi.org/10.1073/pnas.1214704109>  
PMID:[23169648](https://pubmed.ncbi.nlm.nih.gov/23169648/)
20. Chikuma S, Suita N, Okazaki IM, Shibayama S, Honjo T. TRIM28 prevents autoinflammatory T cell development in vivo. *Nat Immunol*. 2012; 13:596–603.  
<https://doi.org/10.1038/ni.2293> PMID:[22544392](https://pubmed.ncbi.nlm.nih.gov/22544392/)
  21. Santos J, Gil J. TRIM28/KAP1 regulates senescence. *Immunol Lett*. 2014; 162:281–89.  
<https://doi.org/10.1016/j.imlet.2014.08.011>  
PMID:[25160591](https://pubmed.ncbi.nlm.nih.gov/25160591/)
  22. Liang Q, Deng H, Li X, Wu X, Tang Q, Chang TH, Peng H, Rauscher FJ 3rd, Ozato K, Zhu F. Tripartite motif-containing protein 28 is a small ubiquitin-related modifier E3 ligase and negative regulator of IFN regulatory factor 7. *J Immunol*. 2011; 187:4754–63.  
<https://doi.org/10.4049/jimmunol.1101704>  
PMID:[21940674](https://pubmed.ncbi.nlm.nih.gov/21940674/)
  23. McNab FW, Rajsbaum R, Stoye JP, O'Garra A. Tripartite-motif proteins and innate immune regulation. *Curr Opin Immunol*. 2011; 23:46–56.  
<https://doi.org/10.1016/j.coi.2010.10.021>  
PMID:[21131187](https://pubmed.ncbi.nlm.nih.gov/21131187/)
  24. Tsuruma R, Ohbayashi N, Kamitani S, Ikeda O, Sato N, Muromoto R, Sekine Y, Oritani K, Matsuda T. Physical and functional interactions between STAT3 and KAP1. *Oncogene*. 2008; 27:3054–59.  
<https://doi.org/10.1038/sj.onc.1210952>  
PMID:[18037959](https://pubmed.ncbi.nlm.nih.gov/18037959/)
  25. Kamitani S, Togi S, Ikeda O, Nakasuji M, Sakauchi A, Sekine Y, Muromoto R, Oritani K, Matsuda T. Krüppel-associated box-associated protein 1 negatively regulates TNF- $\alpha$ -induced NF- $\kappa$ B transcriptional activity by influencing the interactions among STAT3, p300, and NF- $\kappa$ B/p65. *J Immunol*. 2011; 187:2476–83.  
<https://doi.org/10.4049/jimmunol.1003243>  
PMID:[21810609](https://pubmed.ncbi.nlm.nih.gov/21810609/)
  26. Yokoe T, Toiyama Y, Okugawa Y, Tanaka K, Ohi M, Inoue Y, Mohri Y, Miki C, Kusunoki M. KAP1 is associated with peritoneal carcinomatosis in gastric cancer. *Ann Surg Oncol*. 2010; 17:821–28.  
<https://doi.org/10.1245/s10434-009-0795-8>  
PMID:[19898899](https://pubmed.ncbi.nlm.nih.gov/19898899/)
  27. Cui Y, Yang S, Fu X, Feng J, Xu S, Ying G. High levels of KAP1 expression are associated with aggressive clinical features in ovarian cancer. *Int J Mol Sci*. 2014; 16:363–77.  
<https://doi.org/10.3390/ijms16010363>  
PMID:[25548895](https://pubmed.ncbi.nlm.nih.gov/25548895/)
  28. Fitzgerald S, Sheehan KM, O'Grady A, Kenny D, O'Kennedy R, Kay EW, Kijanka GS. Relationship between epithelial and stromal TRIM28 expression predicts survival in colorectal cancer patients. *J Gastroenterol Hepatol*. 2013; 28:967–74.  
<https://doi.org/10.1111/jgh.12157>  
PMID:[23425061](https://pubmed.ncbi.nlm.nih.gov/23425061/)
  29. Liu L, Zhao E, Li C, Huang L, Xiao L, Cheng L, Huang X, Song Y, Xu D. TRIM28, a new molecular marker predicting metastasis and survival in early-stage non-small cell lung cancer. *Cancer Epidemiol*. 2013; 37:71–78.  
<https://doi.org/10.1016/j.canep.2012.08.005>  
PMID:[22959342](https://pubmed.ncbi.nlm.nih.gov/22959342/)
  30. Chen L, Chen DT, Kurtyka C, Rawal B, Fulp WJ, Haura EB, Cress WD. Tripartite motif containing 28 (Trim28) can regulate cell proliferation by bridging HDAC1/E2F interactions. *J Biol Chem*. 2012; 287:40106–18.  
<https://doi.org/10.1074/jbc.M112.380865>  
PMID:[23060449](https://pubmed.ncbi.nlm.nih.gov/23060449/)
  31. Gao J, Aksoy BA, Dogrusoz U, Dresdner G, Gross B, Sumer SO, Sun Y, Jacobsen A, Sinha R, Larsson E, Cerami E, Sander C, Schultz N. Integrative analysis of complex cancer genomics and clinical profiles using the cBioPortal. *Sci Signal*. 2013; 6:p11.  
<https://doi.org/10.1126/scisignal.2004088>  
PMID:[23550210](https://pubmed.ncbi.nlm.nih.gov/23550210/)
  32. Zhou Y, Zhou B, Pache L, Chang M, Khodabakhshi AH, Tanaseichuk O, Benner C, Chanda SK. Metascape provides a biologist-oriented resource for the analysis of systems-level datasets. *Nat Commun*. 2019; 10:1523.  
<https://doi.org/10.1038/s41467-019-09234-6>  
PMID:[30944313](https://pubmed.ncbi.nlm.nih.gov/30944313/)
  33. Selamat SA, Chung BS, Girard L, Zhang W, Zhang Y, Campan M, Siegmund KD, Koss MN, Hagen JA, Lam WL, Lam S, Gazdar AF, Laird-Offringa IA. Genome-scale analysis of DNA methylation in lung adenocarcinoma and integration with mRNA expression. *Genome Res*. 2012; 22:1197–211.  
<https://doi.org/10.1101/gr.132662.111>  
PMID:[22613842](https://pubmed.ncbi.nlm.nih.gov/22613842/)
  34. Chen CH, Lai JM, Chou TY, Chen CY, Su LJ, Lee YC, Cheng TS, Hong YR, Chou CK, Whang-Peng J, Wu YC, Huang CY. VEGFA upregulates FLJ10540 and modulates migration and invasion of lung cancer via PI3K/AKT pathway. *PLoS One*. 2009; 4:e5052.  
<https://doi.org/10.1371/journal.pone.0005052>  
PMID:[19337377](https://pubmed.ncbi.nlm.nih.gov/19337377/)
  35. Hou J, Aerts J, den Hamer B, van Ijcken W, den Bakker M, Riegman P, van der Leest C, van der Spek P, Foekens JA, Hoogsteden HC, Grosveld F, Philipsen S. Gene expression-based classification of non-small cell

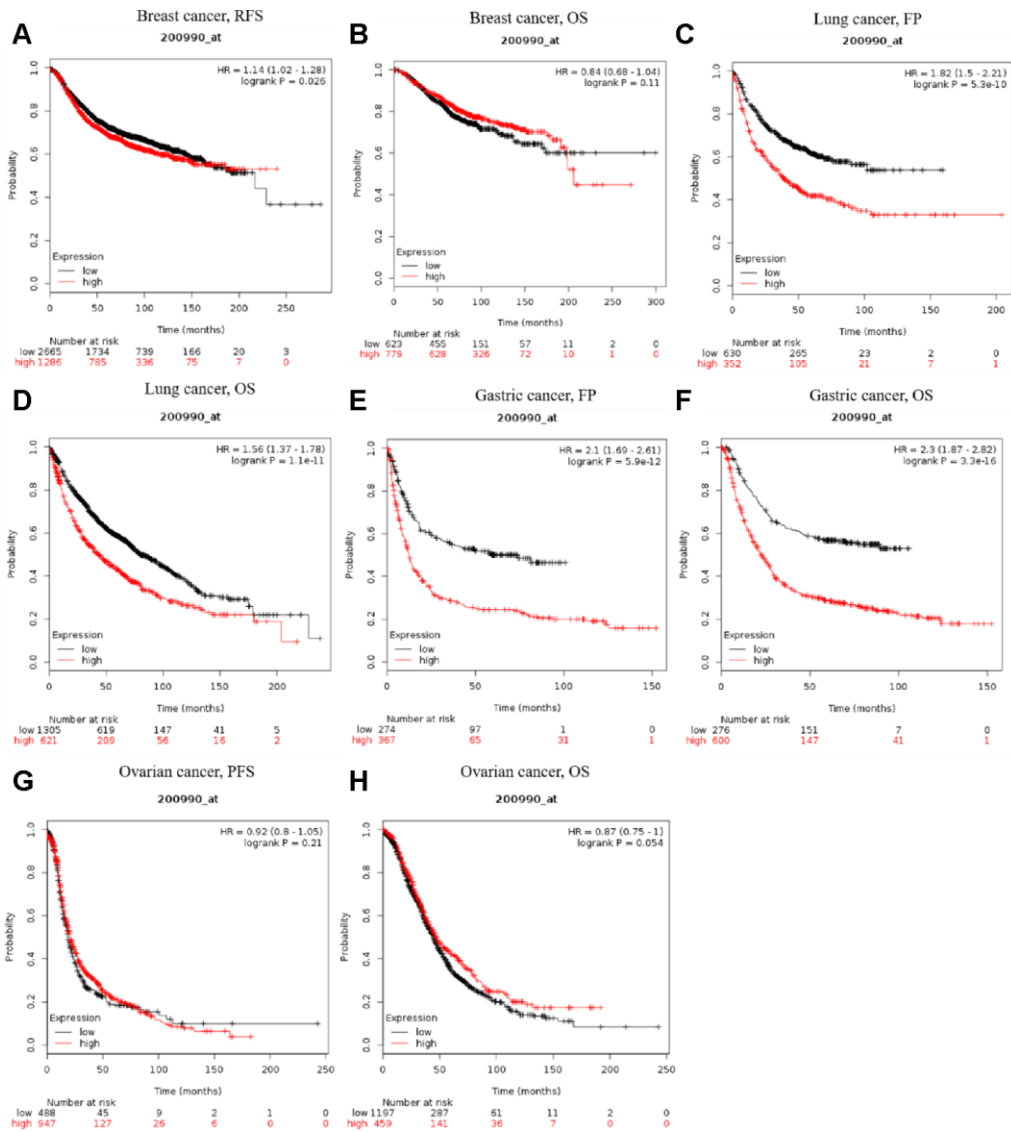
- lung carcinomas and survival prediction. *PLoS One*. 2010; 5:e10312.  
<https://doi.org/10.1371/journal.pone.0010312>  
PMID:[20421987](https://pubmed.ncbi.nlm.nih.gov/20421987/)
36. Beer DG, Kardia SL, Huang CC, Giordano TJ, Levin AM, Misek DE, Lin L, Chen G, Gharib TG, Thomas DG, Lizyness ML, Kuick R, Hayasaka S, et al. Gene-expression profiles predict survival of patients with lung adenocarcinoma. *Nat Med*. 2002; 8:816–24.  
<https://doi.org/10.1038/nm733> PMID:[12118244](https://pubmed.ncbi.nlm.nih.gov/12118244/)
37. Ivshina AV, George J, Senko O, Mow B, Putti TC, Smeds J, Lindahl T, Pawitan Y, Hall P, Nordgren H, Wong JE, Liu ET, Bergh J, et al. Genetic reclassification of histologic grade delineates new clinical subtypes of breast cancer. *Cancer Res*. 2006; 66:10292–301.  
<https://doi.org/10.1158/0008-5472.CAN-05-4414>  
PMID:[17079448](https://pubmed.ncbi.nlm.nih.gov/17079448/)
38. Miller LD, Smeds J, George J, Vega VB, Vergara L, Ploner A, Pawitan Y, Hall P, Klaar S, Liu ET, Bergh J. An expression signature for p53 status in human breast cancer predicts mutation status, transcriptional effects, and patient survival. *Proc Natl Acad Sci USA*. 2005; 102:13550–55.  
<https://doi.org/10.1073/pnas.0506230102>  
PMID:[16141321](https://pubmed.ncbi.nlm.nih.gov/16141321/)
39. Yau C, Benz CC. Genes responsive to both oxidant stress and loss of estrogen receptor function identify a poor prognosis group of estrogen receptor positive primary breast cancers. *Breast Cancer Res*. 2008; 10:R61.  
<https://doi.org/10.1186/bcr2120>  
PMID:[18631401](https://pubmed.ncbi.nlm.nih.gov/18631401/)
40. Chanrion M, Negre V, Fontaine H, Salvetat N, Bibeau F, Mac Grogan G, Mauriac L, Katsaros D, Molina F, Theillet C, Darbon JM. A gene expression signature that can predict the recurrence of tamoxifen-treated primary breast cancer. *Clin Cancer Res*. 2008; 14:1744–52.  
<https://doi.org/10.1158/1078-0432.CCR-07-1833>  
PMID:[18347175](https://pubmed.ncbi.nlm.nih.gov/18347175/)
41. Schmidt M, Böhm D, von Törne C, Steiner E, Puhl A, Pilch H, Lehr HA, Hengstler JG, Kölbl H, Gehrman M. The humoral immune system has a key prognostic impact in node-negative breast cancer. *Cancer Res*. 2008; 68:5405–13.  
<https://doi.org/10.1158/0008-5472.CAN-07-5206>  
PMID:[18593943](https://pubmed.ncbi.nlm.nih.gov/18593943/)
42. Yamauchi M, Yamaguchi R, Nakata A, Kohno T, Nagasaki M, Shimamura T, Imoto S, Saito A, Ueno K, Hatanaka Y, Yoshida R, Higuchi T, Nomura M, et al. Epidermal growth factor receptor tyrosine kinase defines critical prognostic genes of stage I lung adenocarcinoma. *PLoS One*. 2012; 7:e43923.  
<https://doi.org/10.1371/journal.pone.0043923>  
PMID:[23028479](https://pubmed.ncbi.nlm.nih.gov/23028479/)
43. Senovilla L, Vacchelli E, Galon J, Adjemian S, Eggermont A, Fridman WH, Sautès-Fridman C, Ma Y, Tartour E, Zitvogel L, Kroemer G, Galluzzi L. Trial watch: prognostic and predictive value of the immune infiltrate in cancer. *Oncoimmunology*. 2012; 1:1323–43.  
<https://doi.org/10.4161/onci.22009>  
PMID:[23243596](https://pubmed.ncbi.nlm.nih.gov/23243596/)
44. Vasaikar SV, Straub P, Wang J, Zhang B. LinkedOmics: analyzing multi-omics data within and across 32 cancer types. *Nucleic Acids Res*. 2018; 46:D956–63.  
<https://doi.org/10.1093/nar/gkx1090>  
PMID:[29136207](https://pubmed.ncbi.nlm.nih.gov/29136207/)
45. Tarca AL, Lauria M, Unger M, Bilal E, Boue S, Kumar Dey K, Hoeng J, Koepl H, Martin F, Meyer P, Nandy P, Norel R, Peitsch M, et al, and IMPROVER DSC Collaborators. Strengths and limitations of microarray-based phenotype prediction: lessons learned from the IMPROVER diagnostic signature challenge. *Bioinformatics*. 2013; 29:2892–99.  
<https://doi.org/10.1093/bioinformatics/btt492>  
PMID:[23966112](https://pubmed.ncbi.nlm.nih.gov/23966112/)
46. Li Y, Xie P, Lu L, Wang J, Diao L, Liu Z, Guo F, He Y, Liu Y, Huang Q, Liang H, Li D, He F. An integrated bioinformatics platform for investigating the human E3 ubiquitin ligase-substrate interaction network. *Nat Commun*. 2017; 8:347.  
<https://doi.org/10.1038/s41467-017-00299-9>  
PMID:[28839186](https://pubmed.ncbi.nlm.nih.gov/28839186/)
47. Spranger S. Mechanisms of tumor escape in the context of the t-cell-inflamed and the non-T-cell-inflamed tumor microenvironment. *Int Immunol*. 2016; 28:383–91.  
<https://doi.org/10.1093/intimm/dxw014>  
PMID:[26989092](https://pubmed.ncbi.nlm.nih.gov/26989092/)
48. Yaacoub K, Pedoux R, Tarte K, Guillaudeux T. Role of the tumor microenvironment in regulating apoptosis and cancer progression. *Cancer Lett*. 2016; 378:150–59.  
<https://doi.org/10.1016/j.canlet.2016.05.012>  
PMID:[27224890](https://pubmed.ncbi.nlm.nih.gov/27224890/)
49. Giraldo NA, Becht E, Vano Y, Sautès-Fridman C, Fridman WH. The immune response in cancer: from immunology to pathology to immunotherapy. *Virchows Arch*. 2015; 467:127–35.  
<https://doi.org/10.1007/s00428-015-1787-7>  
PMID:[26077464](https://pubmed.ncbi.nlm.nih.gov/26077464/)
50. Wu AA, Drake V, Huang HS, Chiu S, Zheng L. Reprogramming the tumor microenvironment: tumor-induced immunosuppressive factors paralyze T cells.

- Oncoimmunology. 2015; 4:e1016700.  
<https://doi.org/10.1080/2162402X.2015.1016700>  
PMID:[26140242](https://pubmed.ncbi.nlm.nih.gov/26140242/)
51. Otsuka A, Dreier J, Cheng PF, Nägeli M, Lehmann H, Felderer L, Frew IJ, Matsushita S, Levesque MP, Dummer R. Hedgehog pathway inhibitors promote adaptive immune responses in basal cell carcinoma. *Clin Cancer Res*. 2015; 21:1289–97.  
<https://doi.org/10.1158/1078-0432.CCR-14-2110>  
PMID:[25593302](https://pubmed.ncbi.nlm.nih.gov/25593302/)
52. Zaretsky JM, Garcia-Diaz A, Shin DS, Escuin-Ordinas H, Hugo W, Hu-Lieskovan S, Torrejon DY, Abril-Rodriguez G, Sandoval S, Barthly L, Saco J, Homet Moreno B, Mezzadra R, et al. Mutations associated with acquired resistance to PD-1 blockade in melanoma. *N Engl J Med*. 2016; 375:819–29.  
<https://doi.org/10.1056/NEJMoa1604958>  
PMID:[27433843](https://pubmed.ncbi.nlm.nih.gov/27433843/)
53. Tanaka S, Pflieger C, Lai JF, Roan F, Sun SC, Ziegler SF. KAP1 regulates regulatory T cell function and proliferation in both Foxp3-dependent and -independent manners. *Cell Rep*. 2018; 23:796–807.  
<https://doi.org/10.1016/j.celrep.2018.03.099>  
PMID:[29669285](https://pubmed.ncbi.nlm.nih.gov/29669285/)
54. Gehrman U, Burbage M, Zueva E, Goudot C, Esnault C, Ye M, Carpièr JM, Burgdorf N, Hoyler T, Suarez G, Joannas L, Heurtebise-Chrétien S, Durand S, et al. Critical role for TRIM28 and HP1 $\beta/\gamma$  in the epigenetic control of T cell metabolic reprogramming and effector differentiation. *Proc Natl Acad Sci USA*. 2019; 116:25839–49.  
<https://doi.org/10.1073/pnas.1901639116>  
PMID:[31776254](https://pubmed.ncbi.nlm.nih.gov/31776254/)
55. Krischuns T, Günl F, Henschel L, Binder M, Willemsen J, Schloer S, Rescher U, Gerlt V, Zimmer G, Nordhoff C, Ludwig S, Brunotte L. Phosphorylation of TRIM28 enhances the expression of IFN- $\beta$  and proinflammatory cytokines during HPAIV infection of human lung epithelial cells. *Front Immunol*. 2018; 9:2229.  
<https://doi.org/10.3389/fimmu.2018.02229>  
PMID:[30323812](https://pubmed.ncbi.nlm.nih.gov/30323812/)
56. Tsou P, Katayama H, Ostrin EJ, Hanash SM. The emerging role of B cells in tumor immunity. *Cancer Res*. 2016; 76:5597–601.  
<https://doi.org/10.1158/0008-5472.CAN-16-0431>  
PMID:[27634765](https://pubmed.ncbi.nlm.nih.gov/27634765/)
57. Wang SS, Liu W, Ly D, Xu H, Qu L, Zhang L. Tumor-infiltrating B cells: their role and application in anti-tumor immunity in lung cancer. *Cell Mol Immunol*. 2019; 16:6–18.  
<https://doi.org/10.1038/s41423-018-0027-x>  
PMID:[29628498](https://pubmed.ncbi.nlm.nih.gov/29628498/)
58. Gupta P, Chen C, Chaluvally-Raghavan P, Pradeep S. B cells as an immune-regulatory signature in ovarian cancer. *Cancers (Basel)*. 2019; 11:894.  
<https://doi.org/10.3390/cancers11070894>  
PMID:[31248034](https://pubmed.ncbi.nlm.nih.gov/31248034/)
59. Wouters MC, Nelson BH. Prognostic significance of tumor-infiltrating B cells and plasma cells in human cancer. *Clin Cancer Res*. 2018; 24:6125–35.  
<https://doi.org/10.1158/1078-0432.CCR-18-1481>  
PMID:[30049748](https://pubmed.ncbi.nlm.nih.gov/30049748/)
60. Ritchie DS, Yang J, Hermans IF, Ronchese F. B-lymphocytes activated by CD40 ligand induce an antigen-specific anti-tumour immune response by direct and indirect activation of CD8<sup>+</sup> T-cells. *Scand J Immunol*. 2004; 60:543–51.  
<https://doi.org/10.1111/j.0300-9475.2004.01517.x>  
PMID:[15584965](https://pubmed.ncbi.nlm.nih.gov/15584965/)
61. de Visser KE, Korets LV, Coussens LM. De novo carcinogenesis promoted by chronic inflammation is B lymphocyte dependent. *Cancer Cell*. 2005; 7:411–23.  
<https://doi.org/10.1016/j.ccr.2005.04.014>  
PMID:[15894262](https://pubmed.ncbi.nlm.nih.gov/15894262/)
62. Liang J, Wang L, Wang C, Shen J, Su B, Marisetty AL, Fang D, Kassab C, Jeong KJ, Zhao W, Lu Y, Jain AK, Zhou Z, et al. Verteporfin inhibits PD-L1 through autophagy and the STAT1-IRF1-TRIM28 signaling axis, exerting antitumor efficacy. *Cancer Immunol Res*. 2020; 8:952–65.  
<https://doi.org/10.1158/2326-6066.CIR-19-0159>  
PMID:[32265228](https://pubmed.ncbi.nlm.nih.gov/32265228/)
63. Shien K, Papadimitrakopoulou VA, Wistuba II. Predictive biomarkers of response to PD-1/PD-L1 immune checkpoint inhibitors in non-small cell lung cancer. *Lung Cancer*. 2016; 99:79–87.  
<https://doi.org/10.1016/j.lungcan.2016.06.016>  
PMID:[27565919](https://pubmed.ncbi.nlm.nih.gov/27565919/)
64. Rhodes DR, Kalyana-Sundaram S, Mahavisno V, Varambally R, Yu J, Briggs BB, Barrette TR, Anstet MJ, Kincaid-Beal C, Kulkarni P, Varambally S, Ghosh D, Chinnaiyan AM. OncoPrint 3.0: genes, pathways, and networks in a collection of 18,000 cancer gene expression profiles. *Neoplasia*. 2007; 9:166–80.  
<https://doi.org/10.1593/neo.07112> PMID:[17356713](https://pubmed.ncbi.nlm.nih.gov/17356713/)
65. Shannon P, Markiel A, Ozier O, Baliga NS, Wang JT, Ramage D, Amin N, Schwikowski B, Ideker T. Cytoscape: a software environment for integrated models of biomolecular interaction networks. *Genome Res*. 2003; 13:2498–504.  
<https://doi.org/10.1101/gr.1239303>  
PMID:[14597658](https://pubmed.ncbi.nlm.nih.gov/14597658/)
66. Chin CH, Chen SH, Wu HH, Ho CW, Ko MT, Lin CY. cytoHubba: identifying hub objects and sub-networks from complex interactome. *BMC Syst Biol*. 2014 (Suppl

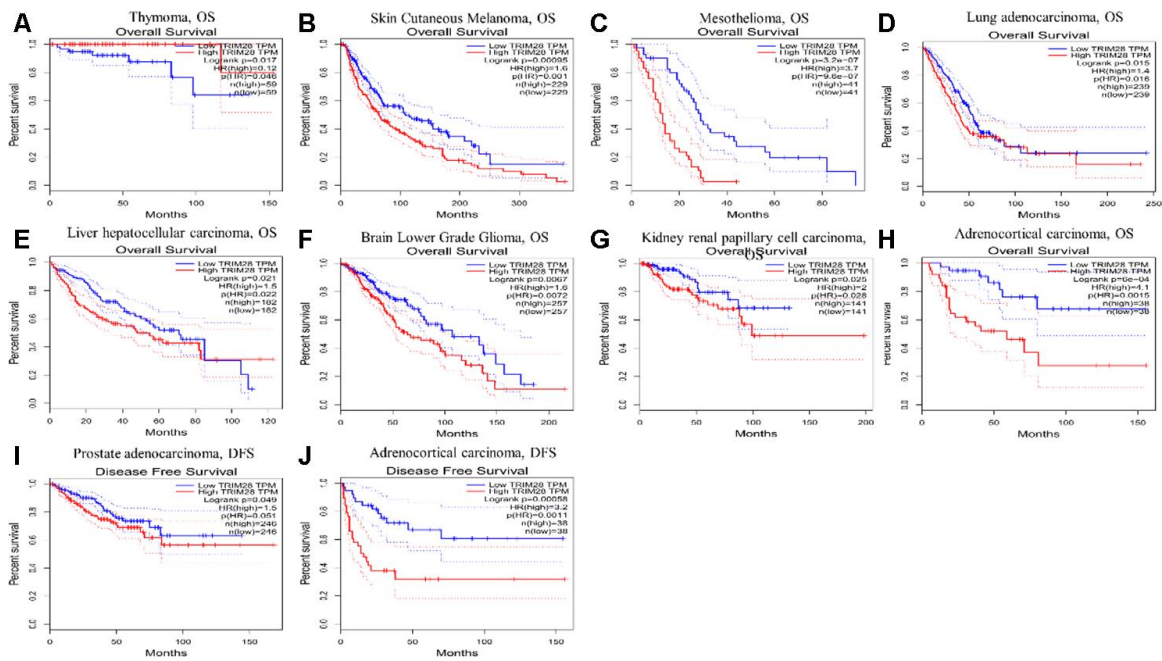
- 4); 8:S11.  
<https://doi.org/10.1186/1752-0509-8-S4-S11>  
PMID:25521941
67. Li T, Fan J, Wang B, Traugh N, Chen Q, Liu JS, Li B, Liu XS. TIMER: a web server for comprehensive analysis of tumor-infiltrating immune cells. *Cancer Res.* 2017; 77:e108–10.  
<https://doi.org/10.1158/0008-5472.CAN-17-0307>  
PMID:29092952
68. Chandrashekar DS, Bashel B, Balasubramanya SA, Creighton CJ, Ponce-Rodriguez I, Chakravarthi BV, Varambally S. UALCAN: a portal for facilitating tumor subgroup gene expression and survival analyses. *Neoplasia.* 2017; 19:649–58.  
<https://doi.org/10.1016/j.neo.2017.05.002>  
PMID:28732212
69. Mizuno H, Kitada K, Nakai K, Sarai A. PrognosScan: a new database for meta-analysis of the prognostic value of genes. *BMC Med Genomics.* 2009; 2:18.  
<https://doi.org/10.1186/1755-8794-2-18>  
PMID:19393097
70. Lániczky A, Nagy Á, Bottai G, Munkácsy G, Szabó A, Santarpia L, Gyórfy B. miRpower: a web-tool to validate survival-associated miRNAs utilizing expression data from 2178 breast cancer patients. *Breast Cancer Res Treat.* 2016; 160:439–46.  
<https://doi.org/10.1007/s10549-016-4013-7>  
PMID:27744485
71. Tang Z, Li C, Kang B, Gao G, Li C, Zhang Z. GEPIA: a web server for cancer and normal gene expression profiling and interactive analyses. *Nucleic Acids Res.* 2017; 45:W98–102.  
<https://doi.org/10.1093/nar/gkx247> PMID:28407145
72. Ru B, Wong CN, Tong Y, Zhong JY, Zhong SS, Wu WC, Chu KC, Wong CY, Lau CY, Chen I, Chan NW, Zhang J. TISIDB: an integrated repository portal for tumor-immune system interactions. *Bioinformatics.* 2019; 35:4200–02.  
<https://doi.org/10.1093/bioinformatics/btz210>  
PMID:30903160
73. Broom BM, Ryan MC, Brown RE, Ikeda F, Stucky M, Kane DW, Melott J, Wakefield C, Casasent TD, Akbani R, Weinstein JN. A galaxy implementation of next-generation clustered heatmaps for interactive exploration of molecular profiling data. *Cancer Res.* 2017; 77:e23–26.  
<https://doi.org/10.1158/0008-5472.CAN-17-0318>  
PMID:29092932

SUPPLEMENTARY MATERIALS

Supplementary Figures



**Supplementary Figure 1. Kaplan-Meier survival curves generated using Kaplan-Meier plotter for TRIM28 expression in different tumor types. (A, B) RFS and OS curves in breast cancer cohorts (n = 1,926, n = 641). (C, D) FP and OS curves in lung cancer cohorts (n = 982, n = 1,926). (E, F) FP and OS curves in gastric cancer cohorts (n = 641, n = 876). (G, H) PFS and OS curves in ovarian cancer cohorts (n = 1,435, n = 1,656). FP, first progression; PFS, Progression-free survival; OS, overall survival; RFS, recurrence-free survival.**



**Supplementary Figure 2.** Kaplan-Meier survival curves generated from the GEPIA database for TRIM28 expression in different tumor types (A–J). DFS, disease-free survival; OS, overall survival. 17. Clinical information data of 517 LUAD patients.

## **Supplementary Tables**

Please browse Full Text version to see the data of Supplementary Tables 1 to 4.

**Supplementary Table 1. Clinical information of 517 LUAD patients.**

**Supplementary Table 2. The immune and stromal scores of 517 LUAD patients.**

**Supplementary Table 3. The hub genes were screened by applying the cytoHubba plugin.**

**Supplementary Table 4. The substrates were predicted by using UbiBrowser.**